



# The role of ATP citrate lyase, phosphoketolase, and malic enzyme in oleaginous *Rhodotorula toruloides*

Alīna Rekēna<sup>1</sup> · Kristjan Pals<sup>1</sup> · Srđan Gavrilović<sup>1</sup> · Petri-Jaan Lahtvee<sup>1</sup>

Received: 5 December 2024 / Revised: 21 February 2025 / Accepted: 11 March 2025  
© The Author(s) 2025

## Abstract

*Rhodotorula toruloides* is an oleaginous yeast recognized for its robustness and the production of high content of neutral lipids. Early biochemical studies have linked ATP citrate lyase (ACL), phosphoketolase (PK), and cytosolic malic enzyme (cMAE) with de novo lipid synthesis. In this study, we discovered that upon a CRISPR/Cas9-mediated knockout of the ACL gene, lipid content in *R. toruloides* IFO0880 decreased from 50 to 9% of its dry cell weight (DCW) in glucose medium and caused severe growth defects (reduced specific growth rate, changes in cell morphology). In xylose medium, the lipid content decreased from 43 to 38% of DCW. However, when grown on acetate as the sole carbon source, the lipid content decreased from 45 to 20% of DCW. Significant growth defects as a result of ACL knockout were observed on all substrates. In contrast, PK knockout resulted in no change in growth or lipid synthesis. Knocking out cMAE gene resulted in lipid increase of 2.9% of DCW and 23% increase in specific growth rate on glucose. In xylose or acetate medium, no change in lipid production as a result of cMAE gene knockout was observed. These results demonstrated that ACL plays a crucial role in lipid synthesis in *R. toruloides* IFO0880, as opposed to PK pathway or cMAE, whose presence in some conditions even disfavors lipid production. These results provided valuable information for future metabolic engineering of *R. toruloides*.

## Key points

- *ACL* is crucial for the fatty acid synthesis and growth in *R. toruloides* IFO0880.
- Lipid production and cell growth is are unchanged as a result of *PK* knockout.
- Cytosolic malic enzyme does not play a significant role in lipogenesis.

**Keywords** Lipid synthesis · ATP citrate lyase · Phosphoketolase · Malic enzyme · *Rhodotorula toruloides*

## Introduction

Oleaginous microorganisms are attractive for the production of biofuels and bio-based oleochemicals from cheap raw materials (Probst et al. 2016; Dourou et al. 2018; Saini et al. 2020; Chawla et al. 2022). Red oleaginous yeast *Rhodotorula toruloides* (*R. toruloides*) is a Basidiomycota fungi that stands out for high lipid content, cell densities, and robustness in consuming hemicellulosic hydrolyzates (Ageitos et al. 2011; Monteiro de Oliveira et al. 2021; Ossorio-González et al. 2022b, 2022a); moreover, it is relatively mature in genetic engineering tools compared to other red

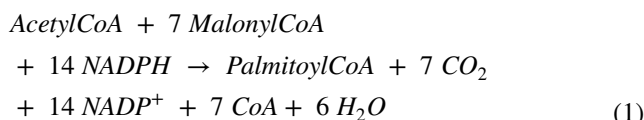
yeasts (Chattopadhyay et al. 2021). Biotechnological applications and prospects of *R. toruloides* as a cell factory are highly promising (Zhao et al. 2022; Yu and Shi 2023; Wu et al. 2023; Sunder et al. 2024). Genomic, transcriptomic, proteomics, and flux balance analyses have established a basic understanding of metabolic pathways and gene functions in *R. toruloides* (Zhu et al. 2012; Coradetti et al. 2018; Dinh et al. 2019; Tiukova et al. 2019a, 2019b; Pinheiro et al. 2020; Kim et al. 2021; Rekēna et al. 2023). Advanced genetic engineering tools have been developed in *R. toruloides* and are being constantly improved. IFO0880 is the best characterized haploid (mating type A2) strain natively producing high titers of neutral lipids up to 8 g/L, reaching lipid content up to 36% of the dry cell weight (DCW) (Zhang et al. 2016b). It is genetically different from another haploid strain NP11 (mating type A1), capable of accumulating similar lipid titers, but significantly higher lipid content (up to 54% of DCW) (Zhu et al. 2012; Zhang et al. 2016b, 2022).

✉ Petri-Jaan Lahtvee  
lahtvee@taltech.ee

<sup>1</sup> Department of Chemistry and Biotechnology, Tallinn University of Technology, Tallinn, Estonia

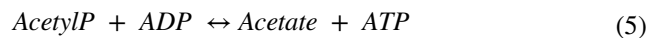
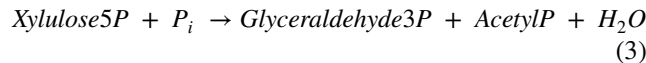
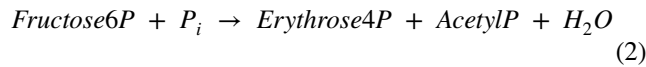
Successful targeted gene deletion with CRISPR has been demonstrated in both IFO0880 and NP11 strains (Otoupal et al. 2019; Jiao et al. 2019; Schultz et al. 2019). The CRISPR/Cas9 offers a simplistic design for targeted (and multiplexed) genome editing (Chattopadhyay et al. 2021). The Cas9 enzyme introduces a double-stranded break in the targeted loci. Precise targeting of the Cas9 endonuclease can be achieved by changing a 20 nucleotide guide RNA (gRNA) sequence (Jinek et al. 2012). Due to lack of plasmid capable of replicating in *R. toruloides* to express CRISPR constructs, existing CRISPR tools in the species are based on a chromosomal integration strategy—stable genome integration of Cas9 and gRNA expression cassette in the chromosome (Otoupal 2019). Several integration plasmids using a selectable drug marker cassette that encodes antibiotic resistance are available (Gong et al. 2024).

One of the most used strategies to enhance lipid production in oleaginous microorganisms is by cultivating cells in secondary nutrient limitation (Wang et al. 2018). An effective way to achieve it is by manipulating nitrogen availability in the culture medium (high C/N ratio) (Papanikolaou and Aggelis 2011; Lopes et al. 2020), but can also be done with manipulating phosphate (Wu et al. 2010) or sulfur concentration (Wu et al. 2011). The main reaction in biosynthesis of fatty acids is carried out by the multi-enzymatic complex of fatty acid synthetase (FAS) in the cytosol. FAS enzyme complex assembles acetyl-CoA and malonyl-CoA into coenzyme A activated fatty acids, such as palmitic acid, using the reducing power from NADPH (Eq. 1) (Tehlivets et al. 2007; Papanikolaou and Aggelis 2011). This is either followed by elongation and desaturation by dedicated enzymes in the endoplasmic reticulum or subsequently used for the acylation of glycerol backbone to synthesize neutral lipids (triacylglycerols, TAGs) (Tehlivets et al. 2007). Accordingly, FAS requires constant supply of acetyl-CoA, malonyl-CoA, and NADPH in cytosol (Beopoulos 2011).



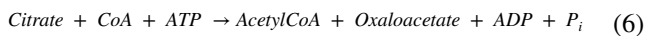
Phosphoketolase (PK) (EC 4.1.2.9) is an enzyme presumed to be one of the candidates to increase acetyl-CoA supply for de novo lipid synthesis. PK is a cytosolic enzyme that cleaves xylulose 5-phosphate or fructose 6-phosphate of the pentose phosphate pathway (PPP) to two-carbon compound acetyl-phosphate and glyceraldehyde 3-phosphate or erythrose 4-phosphate, respectively (Eq. 2 and Eq. 3) (Evans and Ratledge 1984). While acetyl-phosphate will be converted into acetate or acetyl-CoA, the latter two compounds can be recycled via glycolysis and the pentose phosphate pathway (PPP), respectively. On glucose, the involvement of PK in the lipid synthesis was

generally not supported by early biochemical studies with the wild type yeasts (Botham and Ratledge 1979; Boulton and Ratledge 1981). On xylose, there was a strong correlation between PK activity and higher biomass yields demonstrated in wild type *R. toruloides* CBS14 and 14 other yeasts (Evans and Ratledge 1984). Later, it was shown that with overexpression, the native or heterologous PK can enhance lipid production in various yeasts on hemicellulosic carbon sources (Xu et al. 2016; Niehus et al. 2018; Donzella et al. 2019; Kamineni et al. 2021). Based on stoichiometric genome-scale modeling, PPP has been demonstrated as the main glycolytic pathway in *R. toruloides*, while PK playing a crucial role in converting xylulose 5-phosphate into acetyl-phosphate and glyceraldehyde 3-phosphate (Lopes et al. 2020; Rekēna et al. 2023). Omics data show that PK is abundant on glucose, xylose, or acetate in mineral medium (Kim et al. 2021); furthermore, it was significantly upregulated on glucose during lipid accumulation (*p* value 0.043) (Rekēna et al. 2023). From the available genomic data, *R. toruloides* IFO0880 possesses a single PK gene, but is not clear whether the conversion of acetyl-phosphate is catalyzed by phosphate transacetylase, also known as phosphate acetyltransferase (PTA) (EC 2.3.1.8) or acetate kinase (EC 2.7.2.1) (both reversible) (Eq. 4 and Eq. 5) (Dinh et al. 2019; Tiukova et al. 2019b). However, recently engineered NP11 strains overexpressing non-native PTA from bacterial *B. subtilis* demonstrated increased lipid production by up to 15%, increased glucose consumption, and cell mass (Yang et al. 2018).



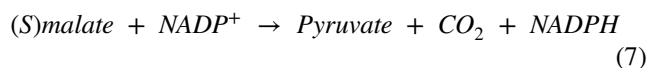
In contrast, ATP citrate lyase (ACL) (EC 2.3.3.8) was associated with lipid synthesis from the early biochemical studies, as its presence correlated to high lipid content in wild type yeasts (Boulton and Ratledge 1981). ACL is a cytosolic enzyme that cleaves cytosolic citrate to acetyl-CoA and oxaloacetate (OAA) (Eq. 6). According to the accepted mechanism for lipid synthesis, ACL activity is associated with the onset of nitrogen limitation that causes excess citrate being exported from the mitochondria to cytosol and used for lipid synthesis under nitrogen limitation (Botham and Ratledge 1979; Boulton and Ratledge 1981). Omics data show that ACL is abundant on glucose, xylose, and acetate in various *R. toruloides* strains, in most of the cases reported as upregulated on proteome level during lipid synthesis and

being more abundant compared to PK (Tiukova et al. 2019a, b; Kim et al. 2021; Rekēna et al. 2023). Also the metabolic engineering studies have shown that ACL plays an important role in lipid biosynthesis in *Ascomycota* yeasts (Liu et al. 2013; Zhang et al. 2014; Sato et al. 2021). In *R. toruloides*, ACL is encoded by a single gene (Zhu et al. 2012), while in ascomycetous yeasts and plants, it has two subunits (Nowrousian et al. 2000; Fatland et al. 2002). Recently, engineered IFO0880 strains overexpressing the ACL gene demonstrated increased fatty alcohol titers (Schultz 2022, Cao et al. 2022). Another possible route to cytosolic acetyl-CoA synthesis from pyruvate is via pyruvate decarboxylase (PDC)—acetaldehyde dehydrogenase—acetyl-CoA synthetase (ACS) path. Previous proteomics studies showed that the abundance of PDC and ACS was low compared to PK and ACL (Rekēna et al. 2023) and downregulated twofold during lipid accumulation (Tiukova et al. 2019a, b); therefore, this pathway was not investigated in this study.



In line with the lipid synthesis mechanism, it was suggested that ACL, FAS, and malic enzyme (MAE) (EC 1.1.1.40) could work together by forming a complex to facilitate fatty acid synthesis (Ratledge 2004; Beopoulos et al. 2011). Because ACL catalyzes the conversion of citrate into acetyl-CoA and OAA, the latter can be transformed into malate and further converted into pyruvate by MAE, simultaneously reducing NADP(+) into NADPH (Eq. 7); thus, MAE may also play an important role to supply of the reducing power for fatty acid synthesis. Several metabolic engineering studies confirmed the hypothesis of the role of MAE in filamentous fungi, like *Mucor circinelloides* (Wynn et al. 1997; Zhang et al. 2007), *Mortierella alpina* (Wynn et al. 2001), and *Aspergillus nidulans* (Wynn and Ratledge 1997), suggesting that malic enzyme was one of the rate-limiting steps for fatty acid synthesis. However in similar studies with the oleaginous ascomycetous yeast *Yarrowia lipolytica* and basidiomycetous yeast *Rhodotorula glutinis*, it did not perform the same way (Yoon et al. 1984; Zhang et al. 2013; Blazeck et al. 2014; Wasyleenko et al. 2015; Dulermo et al. 2015; Qiao et al. 2017; Zhu et al. 2023). Namely, it resulted in a current understanding that oleaginous yeasts are different from filamentous fungi, and the primary sources of cytosolic NADPH are glucose 6-phosphate dehydrogenase (G6PD, also known as ZWF) and 6-phosphogluconate dehydrogenase of the PPP, and isocitrate dehydrogenase (Chawla et al. 2022; Sreeharsha and Mohan 2020; Yang et al. 2012; this study), an alternative route being via cytosolic malic enzyme only while growing on substrates that are not catabolized via glycolytic pathways. Both ZWF and MAE are abundant in *R. toruloides* in mineral medium on glucose, xylose, or acetate, but the results of their differential expression

during lipid synthesis are inconclusive among the studies (Tiukova et al. 2019a, b; Kim et al. 2021; Rekēna et al. 2023). The observed higher abundance of oxPPP enzymes suggests their primary role in NADPH regeneration, but it was not investigated further due to report on gene essentiality from a previous study (Coradetti et al. 2018). Moreover, the deletion of MAE would tell if the other pathway prevailed, as these are the two main candidate pathways for the regeneration of NADPH in *R. toruloides*. It should be noted that *Y. lipolytica* possesses only a mitochondrial MAE (mMAE), while *R. toruloides* holds both cytosolic and mitochondrial forms of MAE (Zhu et al. 2012; Coradetti et al. 2018). Engineered IFO0880 strains overexpressing native cytosolic MAE (cMAE) enzyme demonstrated a minor increase in lipid synthesis on glucose (Zhang et al. 2016a). A heterologous overexpression of MAE from *Y. lipolytica* did not increase the expression of fatty alcohols in *R. toruloides* IFO0880 (Schultz et al. 2022). The role and cofactor dependency of the *R. toruloides* mMAE form still remains unclear. mMAE was not investigated in this study.



Taken altogether, to clarify whether PK, ACL, and cMAE contributes to the lipid biosynthesis in *R. toruloides*, the latest CRISPR/Cas9 tool was used for a targeted single gene knockout of PK, ACL, and cMAE in a wild type IFO0880. Cell growth and lipid production in the knockout strains were examined. To understand the substrate-dependent differences, the knockouts were characterized in a chemically defined medium at nitrogen limitation (C/N 80) on glucose, xylose, and acetic acid as a sole carbon sources. The study revealed very different physiological responses between these genes and lipid synthesis, providing valuable insights in *R. toruloides* metabolism, building understanding relevant for the future metabolic engineering. ACL knockout strain demonstrated the most severe effect on the growth and lipid production on all the characterized substrates while  $\Delta\text{PK}$  and  $\Delta\text{cMAE}$  strains demonstrated less severe physiology differences in comparison to the wild type strain. This is the first study of these gene knockouts in *R. toruloides*.

## Materials and methods

### Strains, media, and conditions

Routine growth *R. toruloides* was performed in YPD medium (10 g/L yeast extract, 20 g/L peptone, and 20 g/L glucose).

For selection or maintenance of transformants, 200 µg/mL G418 (Gibco) was added to the YPD medium.

Lipid content was measured in cells grown in a low-nitrogen mineral medium. Basal medium contained 3.0 g/L  $\text{KH}_2\text{PO}_4$ , 0.5 g/L  $\text{MgSO}_4 \cdot 7\text{H}_2\text{O}$ , 15 mg/L EDTA, 4.5 mg/L  $\text{ZnSO}_4 \cdot 7\text{H}_2\text{O}$ , 0.3 mg/L  $\text{CoCl}_2 \cdot 6\text{H}_2\text{O}$ , 1 mg/L  $\text{MnCl}_2 \cdot 4\text{H}_2\text{O}$ , 0.3 mg/L  $\text{CuSO}_4 \cdot 5\text{H}_2\text{O}$ , 4.5 mg/L  $\text{CaCl}_2 \cdot 2\text{H}_2\text{O}$ , 3 mg/L  $\text{FeSO}_4 \cdot 7\text{H}_2\text{O}$ , 0.4 mg/L  $\text{Na}_2\text{MoO}_4 \cdot 2\text{H}_2\text{O}$ , 1 mg/L  $\text{H}_3\text{BO}_3$ , 0.1 mg/L KI, 0.05 mg/L biotin, 1 mg/L calcium pantothenate, 1 mg/L nicotinic acid, 25 mg/L inositol, 1 mg/L thiamine HCl, 1 mg/L pyridoxine HCl, and 0.2 mg/L para-aminobenzoic acid (Verduyn et al. 1992). Basal medium was supplemented with 20 g/L glucose (Roth), or 20 g/L xylose, or 10 g/L acetate (Chempur) as a sole carbon source. Ammonium sulfate  $(\text{NH}_4)_2\text{SO}_4$  was used as a nitrogen source to obtain a C/N ratio of 80 (mol/mol); 0.55 g/L of  $(\text{NH}_4)_2\text{SO}_4$  (Fisher Bioreagents) was added to the medium containing glucose or xylose, and 0.275 g/L  $(\text{NH}_4)_2\text{SO}_4$  was added to the medium containing acetate. For adjusting the media containing glucose or xylose, 5.2 g/L  $\text{K}_2\text{HPO}_4$  (Roth) was added (pH 5.8 to 8.0). The potassium phosphate buffer did not sustain the pH with 10 g/L of acetate in the medium; therefore, instead, it was adjusted to a starting pH 6 with 2 M KOH (Thermo Fisher Scientific).

*Escherichia coli* strain TOP10 (Thermo Fisher Scientific) was used for plasmid assembly and routine cloning. The strain and its derivatives were grown in Luria Broth (LB) medium at 37 °C and 200 rpm with 50 µg/mL kanamycin.

Unless differently stated, all other reagents were purchased from Sigma-Aldrich Co., St Louis, MO, USA.

## DNA sequences

DNA sequences of *R. toruloides* IFO0880 strain were obtained from MycoCosm database (*R. toruloides* v4.0) (JGI) (Coradetti et al. 2018). Genes with accession numbers 9725 (ATP citrate lyase, ACL) and 13,382 (phospho-ketolase, PK) were retrieved and used to design the guide RNAs, as there were no other alternative genes with a similar sequence. Based on the annotation found from the two existing genome-scale models, gene with accession number 12761 was retrieved and used to design gRNAs to target the cytosolic, NADP-dependent malic enzyme (cMAE) (Tiukova et al. 2019b; Kim et al. 2021). The single gRNAs targeting the first exon 1 of ORF of the target gene (exon 5 in case of the ACL gene) were designed with the CCTop online tool using *Ganoderma lucidum* as the reference genome (Stemmer et al. 2015). 23-nucleotide target sequence ending with NGG (*Streptococcus pyogenes*) and set custom overhangs (forward strand 5' CGCA and reverse strand 5' AAC) was selected based on the CRISPRater efficacy score (Labuhn et al. 2018) above 74 (high efficacy).

Oligonucleotides without the NGG 3-mer (20-nucleotide target sequence + overhangs) were synthesized by IDT (Integrated DNA Technologies, Leuven, the Netherlands).

## Guide RNA cloning

The plasmid pPBO.202 for CRISPR/Cas9-mediated genome editing of *R. toruloides* IFO0880 was obtained from the JBEI Registry <https://registry.jbei.org/> (part ID JBEI223791). pPBO.202 contained constructs for a functional expression of the CRISPR/Cas9 system in *R. toruloides*. They were optimized by Otoopal and colleagues (Otoopal et al. 2019) to be as follows: (i) *E. coli* elements of ColE1 (KanR promoter, kanamycin resistance), (ii) a gRNA expression cassette with *R. toruloides* fusion 5S rRNA-tRNA<sup>Phe</sup> promoter, 2 *Bsa*I sites, the *S. cerevisiae* SUP4 terminator, (iii) a codon optimized SpCas9 expression cassette with IFO0880 GPD1 promoter and NOS terminator, and (iv) *R. toruloides* G418 resistance cassette ptUB2-G418-tTUB2. Two oligos with a forward strand 5' CGCA and reverse strand 5' AAC overhang were annealed and subsequently cloned by digesting plasmid pPBO.202 with *Bsa*I (Thermo Fisher Scientific) and ligating in T4 Ligase buffer (Thermo Fisher Scientific) in a single pot reaction. Plasmid cloning was performed in *Escherichia coli* strain TOP10 (Thermo Fisher Scientific) according to the manufacturer's instructions, and bacterial plasmid DNA was purified using FavorPrep Mini Plasmid Kit (FAVORGEM, Ping Tung, Taiwan). Resulting plasmids pPBO.202–13382(3), pPBO.202–9725(1), and pPBO.202–12761(1) were checked by Sanger sequencing. Several different gRNAs per target gene were tested in sequential order if the previous gRNA candidate failed to result in the target site disruption (the number in the brackets next to each construct indicates the number of different gRNA test candidates that resulted in a functional CRISPR/Cas9 mediated target site disruption).

## Yeast transformation

Yeast transformation was performed using lithium acetate/PEG-mediated chemical transformation method as previously described (Tsai et al. 2017; Bonturi et al. 2022). Briefly, cells from an overnight YPD culture were inoculated at OD<sub>600</sub> 0.2 in a shake flask containing 50 mL of YPD (for up to 10 transformations). At OD<sub>600</sub> 0.8, cells were harvested, washed in dH<sub>2</sub>O, and eventually mixed with 240 µL PEG 4000 (Fisher Scientific), 36 µL 1 M LiAc pH 7.5 (Alfa Aesar), 24 µL dH<sub>2</sub>O, 10 µL pre-boiled Salmon Sperm (10 mg/mL), and 0.1–10 µg purified circular plasmid DNA dissolved in 50 µL of water. The mixture was incubated at 30 °C shaking for 30 min, added with 34 µL of DMSO and heat shocked at 42 °C for 15 min. After removing the supernatant, collected cells were resuspended in 2 mL of YPD and incubated at 30 °C overnight for the recovery. Then, cells were collected, spread on YPD agar plates (agar 20 g/L) the selective antibiotic 200 µg/mL G418, and incubated at 30 °C for 2–4 days until the colonies appeared.

## Isolation of gene knockouts

Multi-step verification was used to confirm target gene inactivation: (i) antibiotic selection, (ii) genomic DNA isolation using lithium acetate/SDS/heat lysis (Looke et al. 2011) and Cas9-specific PCR on the genomic DNA, (iii) target gene PCR amplification and sequencing. PCR amplification at the target locus of PK was performed with primers 5' CCTCCCTCTCACTCTGCAC '3 (forward) and 5' CACGCTGTCCAGTCAAAGAA '3 (reverse); ACL—with primers 5' AGCTCCTCAAGCACGTCACT '3 (forward) and 5' GTAGACGACCGAACGACCCAC '3 (reverse), and MAE—with primers 5' ACTCGCTCTCCCTCTCTC '3 (forward) and 5' ACTCGGAAAACCACGGCTTC '3 (reverse). It was performed using high-fidelity Platinum SuperFi II DNA Polymerase Green PCR Master Mix (2X) (Thermo Fisher Scientific, Vilnius, Lithuania) according to manufacturer's instructions for a high GC content template. PCR amplification of the Cas9 coding sequence with primers 5' GGAGTCGGGGACGCCAAC '3 (forward) and 5' ACACGTTGGCGTCCCCGGA '3 (reverse) was performed using DreamTaq Polymerase Green PCR Master Mix (2x) (Thermo Fisher Scientific, Vilnius, Lithuania). PCR DNA was purified using FavorPrep Mini Gel/PCR Kit (FAVORGREN, Ping Tung, Taiwan).

## Physiological characterization

The seed culture from a fresh YPD agar plate was inoculated to a sterile 250-mL baffled Erlenmeyer flask filled with 25 mL of YPD. After 19 h at 30 °C and 200 rpm, sufficient amount of broth was transferred to a sterile 50 mL Falcon tube and pelleted (5000 g, 5'). After discard of supernatant, cell pellet was washed twice with a sterile dH<sub>2</sub>O and used to inoculate 10 mL of low-nitrogen mineral medium at OD<sub>600</sub> of 0.5 in aerobic 50 mL Biosan RTS-8 Multi-channel falcon tube bioreactors (Biosan, Riga, Latvia). Calibration curves for OD quantification were prepared in a range between OD<sub>600</sub> 0 and 55 with 8 calibration points using *R. toruloides* shake flask culture in a chemically defined medium. Calibration curves for pH and dO measurement were set up according to the manufacturer's instructions. Real-time logging was set to every 30 min with RTS-8 proprietary software. Agitation speed was set to 2500 rpm, temperature 30 °C. Every 12 h after the cells had reached the exponential growth phase, except for the first sample after time point zero, samples to measure offline OD<sub>600</sub> and extracellular metabolites were withdrawn from the bioreactor tube in the laminar flow cabinet, transferred to a 2-mL Eppendorf tubes and centrifuged for 5' at 11,000 × g. The supernatant was collected and stored at –20 °C for further analysis. The first sample was collected 6 h after inoculation. All cultivations

were carried out in a batch regime; no feed was added throughout the process. All samples were collected from three independent replicates for each experimental condition, i.e., combination of strain and carbon source. Specific growth rate was calculated by fitting an exponential trend line to the real time OD data using Eq. 8 with MS Excel software.

$$OD(t) = OD_0 \times e^{\mu t} \quad (8)$$

where  $OD_0$  is the initial optical density,  $t$  is elapsed time,  $\mu$  is the specific growth rate,  $OD(t)$  is the resulting optical density at time  $t$ .

## Lipid analysis

At the end of the cultivation experiment, cell broth containing at least 12 mg of DCW was transferred from the falcon tube bioreactor to a 15 mL tube and separated by centrifugation (5000 g, 10', 4 °C). Cell pellets were frozen at –80 °C, lyophilized, and stored at –20 °C until further analysis. To quantify lipids, fatty acids were extracted and derivatized by using one-step method as described by Sukhija and Palmquist (Sukhija and Palmquist 1988), with internal standard heptadecanoic acid (17:0) solution in toluene (5 mg/mL). Fatty acids were analyzed using Agilent (Santa Clara, CA, USA) 6890 A gas chromatograph equipped with a flame ionization detector (GC-FID). The column was a quartz capillary column (100 m × 0.25 mm) with liquid phase CP-Sil 88, temperature programmed from 70 to 180 °C at 13 °C/min, held for 40 min, 180 to 225 °C at 5 °C/min, held for 15 min. Hydrogen was used as the carrier gas for GC and FID (FID flow rate 30 mL/min), air flow rate 300 mL/min. Fatty acids were identified by comparison of their retention times with the retention time of mixtures with known fatty acid methyl ester composition and concentration: Supelco 37 Component FAME Mix (Sigma-Aldrich Co., St Louis, MO, USA), Nu-Chek Prep CLC 603, and Nu-Chek Prep CLC 428 (Nu-Chek Prep Inc., Elysian, MN, USA). Fatty acid composition was presented as a gram of individual fatty acids per 100 g of total fatty acids (the same as relative %). Lipid content was calculated as the weight sum of individual fatty acids in 100 g of sample, divided by 0.9 to provide TAG equivalent known from earlier biochemical studies, as described by Sukhija and Palmquist (1988), and expressed as gram lipids per gram dry cell weight (DCW). Non-lipid cell mass was calculated after subtraction of intracellular lipids from cell mass.

## Analytical methods

Extracellular metabolites in cultivation broth were measured using HPLC (LC-2050C, Shimazu, Kyoto, Japan) equipped with a refractive index detector and a variable wavelength

detector. Prior analysis, all samples were thawed, filtered (0.22 µm), and diluted in an appropriate diluent as indicated below. Metabolites were analyzed using the Aminex HPX-87H 300×7.8 mm column (Bio-Rad, Hercules, CA, USA) at 45 °C, with 5 mM H<sub>2</sub>SO<sub>4</sub> as the mobile phase with isocratic elution at 0.6 mL/min. The concentrations of acetate, glucose, glycerol, xylose, citrate, xylitol, and D-arabitol were quantified by refractive index detector based on the calibration curves prepared in the range between 0.625 and 20 g/L. No unknown peaks by variable wavelength detector set at 210 nm were detected. It should be noted that with the HPX-87H, it is not possible to determine the chirality of arabitol, but we have determined it in our previous publication (Rekēna et al. 2023). To adjust the sample volume, samples containing glucose or xylose were diluted to 5X in ultrapure H<sub>2</sub>O (Milli-Q Ultrapure Water System, Merck, Darmstadt, Germany). To adjust the pH and the volume, samples containing acetate were diluted to 5X in 10 mM mobile phase to reduce the pH below 8, the maximum range of the column. Biomass optical density data were calibrated by gravimetric dry cellular mass measurements. The linearly fitted calibration coefficient was 0.3 for cells under the exponential growth and 0.26 for cells under nitrogen limitation. At the end of cultivation, 3 uL of culture were transferred to a glass slide for microscopy. Cells from an undiluted culture were visualized by a bright-field microscope under 100× magnification CX21 (Olympus, Tokyo, Japan). All images were acquired using Apple iPhone 13 mini (Apple Inc., Cupertino, CA, USA).

## Statistical analysis

Statistical analysis of physiological parameters evaluation was performed using GraphPad Prism 9.5.1 (GraphPad Software Inc., San Diego, CA, USA). Statistical significance was calculated using one-way ANOVA (Analysis of variance) at 0.05 significance level. *p*-values were adjusted (apval) for multiplicity following Dunnett multiple comparison testing against the wild type IFO0880.

## Results

### Sequencing of the genomic DNA confirmed gene knockouts introduced by CRISPR/Cas9

Gene knockouts were introduced into the *R. toruloides* IFO0880 genome by using a one-step CRISPR/Cas9 strategy. The coding sequence of the Cas9 and appropriate gRNAs were randomly integrated into the genome through use of a single plasmid vector pPBO.202 (JBEI Registry part ID JBEI223791) with the G418 selection marker using lithium acetate/PEG-mediated chemical transformation (see

**Table 1** List of gRNAs used in this study. Number in the brackets refers to number of different gRNA needed to be tested in order to successfully generate the gene knockout

gRNA	Target gene	Target sequence (5'-3')
9725(1)	ACL	AGTACGTCGTCGGTCCCAAG
13382(3)	PK	GATGCAGAGGAAGTTGACCA
12761(1)	cMAE	CCCTCCCAGCCCCTCAAGG

“Materials and Methods”). A set of single guide RNAs targeting PK, ACL, or cMAE were designed to separately target and disrupt the first exon of the targeted genes (Table 1). Gene knockouts by CRISPR/Cas9 were confirmed by sequencing of the genomic DNA around the gRNA-targeted cut site. Mutations at the site targeted by the gRNAs were identified by aligning sequences against the wild type *R. toruloides* IFO0880 reference genome (Fig. 1a). In case of ACL knockout, there was a visible phenotypic difference (Fig. 1b). Other knockouts did not display a phenotypic difference. The gene knockouts by CRISPR/Cas9 were presumably generated by sequence of Cas9 endonuclease and error prone NHEJ DNA repair resulting in frameshift mutation in wild type *R. toruloides* strain. It has been reported that the frequency of HR in *R. toruloides* is low (Koh et al. 2014). List of strains used in this study is provided in Table 2; number of clones screened is reported in Supplementary Table S1.

During the strain characterization step, growth curves (in the next section) of wild type cells and cells harboring gene editing vector did not show difference in growth rates. No significant differences in growth rates were observed between different mutation variants of cMAE and PK during initial screening. This shows that cassette did not cause detrimental fitness effects, similarly as reported by Otoupal and colleagues (Otoupal et al. 2019). These results demonstrated that it is possible to achieve the disruption of central carbon metabolism genes with a method that relies on a stable genome integration of CRISPR constructs in the genome using a selectable drug marker.

### ACL knockout decreases lipid synthesis on glucose

To understand the role of PK, ACL, and cMAE in the lipid synthesis of *R. toruloides* IFO0880 strain, we compared the lipid content produced by the knockout strains versus the wild type IFO0880. Cells were induced for lipid production using low-nitrogen mineral medium containing glucose, xylose, or acetate as a solo carbon source. *R. toruloides* is an obligate aerobe. For the best mixing and aeration support, high-throughput falcon tube bioreactors equipped with a reverse-Spin® technology RTS-8 (Biosan, Riga, Latvia) instead of shaker flasks or traditional stirred tank bioreactors

were used for strain characterization. This system was not equipped with the option to maintain desired pH and dissolved oxygen settings, but provided for a real time non-invasive tracking of OD, pH, and dissolved oxygen data. We used real-time dissolved oxygen monitoring to precisely track the end of the experiment. To account for the pH drop happening with *R. toruloides* in an uncontrolled pH environment (Tingajeva 2024), K<sub>2</sub>HPO<sub>4</sub> was added in the starting media at pH 6.5 to an amount sufficient to buffer significant pH changes (see “Materials and Methods”).

On glucose, online OD<sub>600</sub> data showed no difference among the strains in the lag phase prior to the exponential growth phase (Fig. 2a), but the maximum specific growth rate of the ACL knockout was significantly decreased by 41% as compared to the wild type strain (Fig. 2b, Supplementary Table S2, apval < 0.002). The growth of the ACL mutant continued until 18 h, but then the growth stopped and final DCW did not reach that of the wild type strain (Fig. 2c). Sugar analysis confirmed that the ΔACL stopped consuming glucose after 18 h (Fig. 2d). The pH remained within the optimal range throughout the cultivation (Supplementary

Fig. S1). The dissolved oxygen curves showing when the end of the experiment was declared are available from Supplementary Fig. S2.

For lipid quantification, we used gas chromatographic (GC) determination (see “Materials and Methods”). In the wild type strain, lipid content reached 50.18 ± 0.37% (g lipid per g of DCW) after 54 h of growth on low-nitrogen mineral media (Table 3). The ACL knockout strain showed a significant decrease in lipid content by 81% compared to the wild type strain, reaching only 9.43 ± 0.039% (g<sub>lipid</sub>/g<sub>DCW</sub>) (Fig. 2e, apval < 0.0001). In case of the ACL knockout, the difference in non-lipid DCW (g/L) compared to the wild type strain was 58% (apval < 0.0001) (Supplementary Fig. S3a). These results indicated that ACL was not only essentially involved in *R. toruloides* fatty acid synthesis, similarly as previously studied in *Y. lipolytica* and *L. starkeyi* (Dulermo et al. 2015; Liu et al. 2013; Sato et al. 2021), but also involved in some other essential processes that had a complementary effect on cellular physiology, whereas knocking out the PK gene showed no change in specific growth rate or lipid content, suggesting PK had no major

**Fig. 1** Examples of targeted gene disruption using CRISPR/Cas9. Only one example shown per targeted gene. **a** Partial sequencing of phosphoketolase (PK), ATP citrate lyase (ACL), and cytosolic malic enzyme (cMAE) of one edited colony near the cut site in the targeted genes. **b** Phenotype comparison of wild type *R. toruloides* IFO0880 versus ΔACL, ΔPK, and ΔcMAE strains after 9 days growth on YPD agar

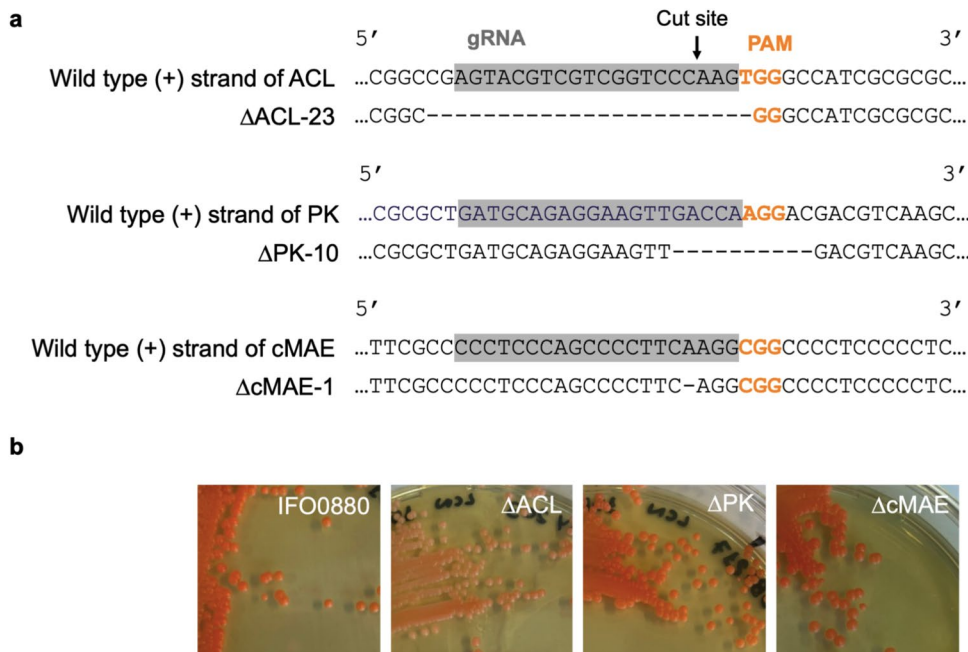


**Table 2** List of strains used in this study

Strain name	Genotype	Parent strain	Antibiotic	Mutation	Source/reference
IFO0880 (NBRC 0880)	<i>Rhodotorula toruloides</i> strain IFO0880 (now NBRC 0880), mating type A2	N/A	N/A	N/A	NBRC collection
ΔACL	pPBO.202-9725(1)	IFO0880	G418	23 bp deletion	This study
ΔPK	pPBO.202-13382(3)	IFO0880	G418	10 bp deletion	This study
ΔcMAE	pPBO.202-12761(1)	IFO0880	G418	1 bp deletion	This study

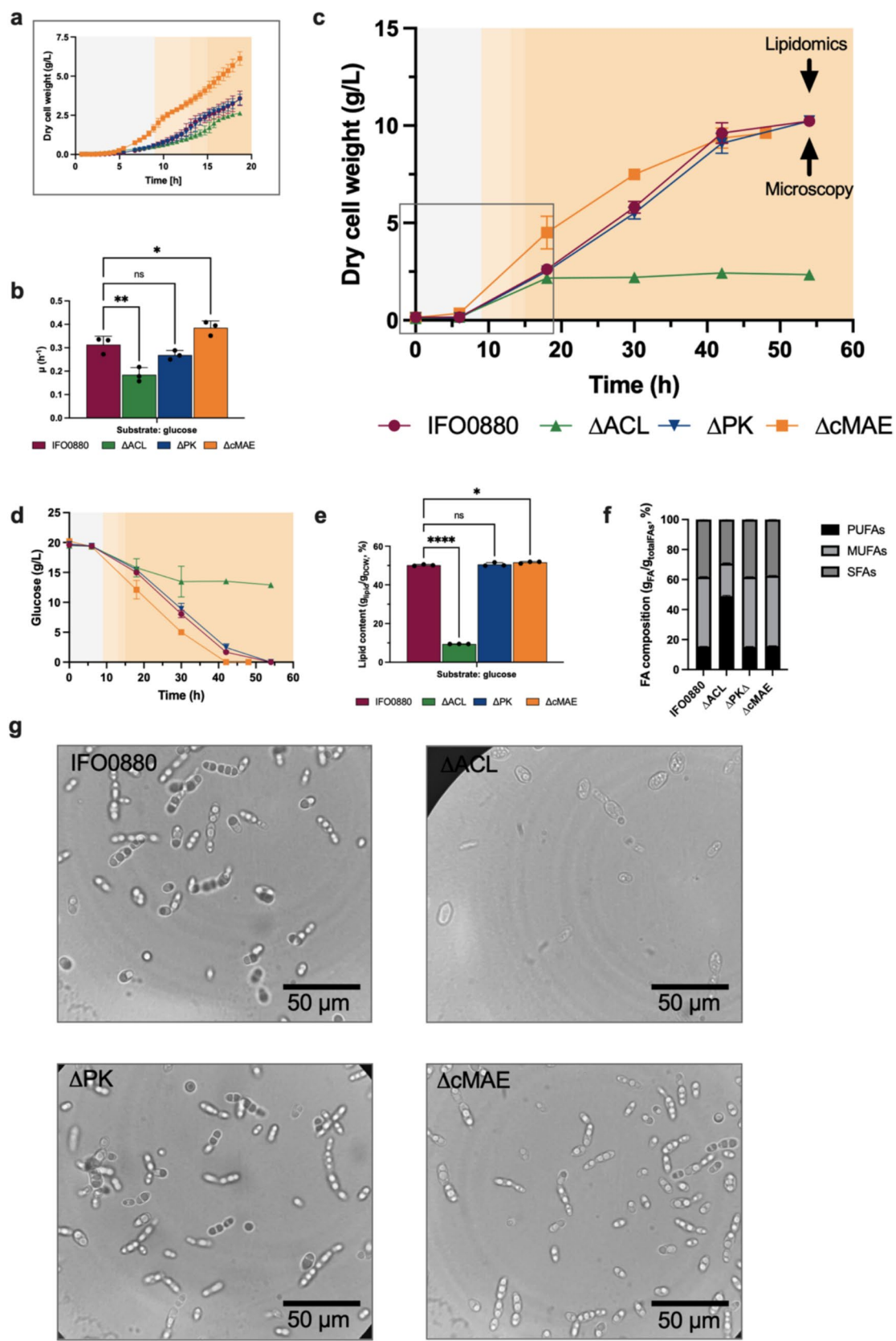


**Fig. 2** Physiological parameters obtained in glucose-based pH-adjusted low-nitrogen mineral medium (C/N ratio 80) (Verduyn et al. 1992). Data obtained from cultivating *R. toruloides* wild type IFO0880 (circle), ATP citrate lyase knockout ( $\Delta$ ACL, pyramid), phosphoketolase knockout ( $\Delta$ PK, inverted pyramid), and cytosolic malic enzyme knockout ( $\Delta$ cMAE, square) strains in falcon tube bioreactors with non-invasive OD, dO<sub>2</sub>, and pH sensors. **a** A snapshot of the online OD<sub>600</sub> data displayed as the dry cell weight (g/L), **b** maximum specific growth rate fitted from the exponential growth phase OD<sub>600</sub> data (h<sup>-1</sup>), **c** dry cell weight (g/L), **d** substrate concentration (g/L), **e** lipid content (g<sub>lipid</sub>/g<sub>DCW</sub>, %); cells harvested at the end of cultivation, **f** relative fatty acid composition (g<sub>FA</sub>/g<sub>totalFAs</sub>, %); cells harvested at the end of cultivation, **g** morphology comparison of wild type IFO0880 versus knockout strains visualized by bright-field microscope, cells harvested at the end of cultivation. Panels **a** and **c** background colors denote the switch in growth phases based on dO<sub>2</sub> curves available from Supplementary Fig. S2, presumably pointing to the onset of the nitrogen limitation phase. FAs fatty acids, SFAs saturated fatty acids, MUFA monounsaturated fatty acids, PUFA polyunsaturated fatty acids. Error bars are calculated as a standard deviation from three biological experiments. Asterisks denote statistical significance (ANOVA Dunnett's multiple comparison test against the wild type IFO0880 strain, adjusted *p* value \**p*<0.05, \*\**p*<0.01, \*\*\**p*<0.001, \*\*\*\**p*<0.0001). ns is used to denote changes that are statistically nonsignificant

effect on growth or lipid synthesis under the studied environmental conditions (Fig. 2a–f). In contrast, the specific growth rate of  $\Delta$ cMAE was increased by 23% compared to the wild type strain, reaching  $0.39 \pm 0.030$  h<sup>-1</sup> (Fig. 2b, *p*val 0.04). Lipid content of  $\Delta$ cMAE increased by 2.9% of DCW compared to the wild type strain (*p*val 0.03), but no significant changes in the fatty acid profile were observed (Fig. 2e). These results indicated that cMAE in *R. toruloides* is not essential in lipid biosynthesis under the studied environmental conditions. Previously, it was reported in oleaginous *Y. lipolytica* that the deletion of mMae in the wild type strain has no effect on lipid content or fatty acid profiles (Blazeck et al. 2014; Dulermo et al. 2015; Zhu et al. 2023). However, only the deletion of cMAE was studied in the present work.

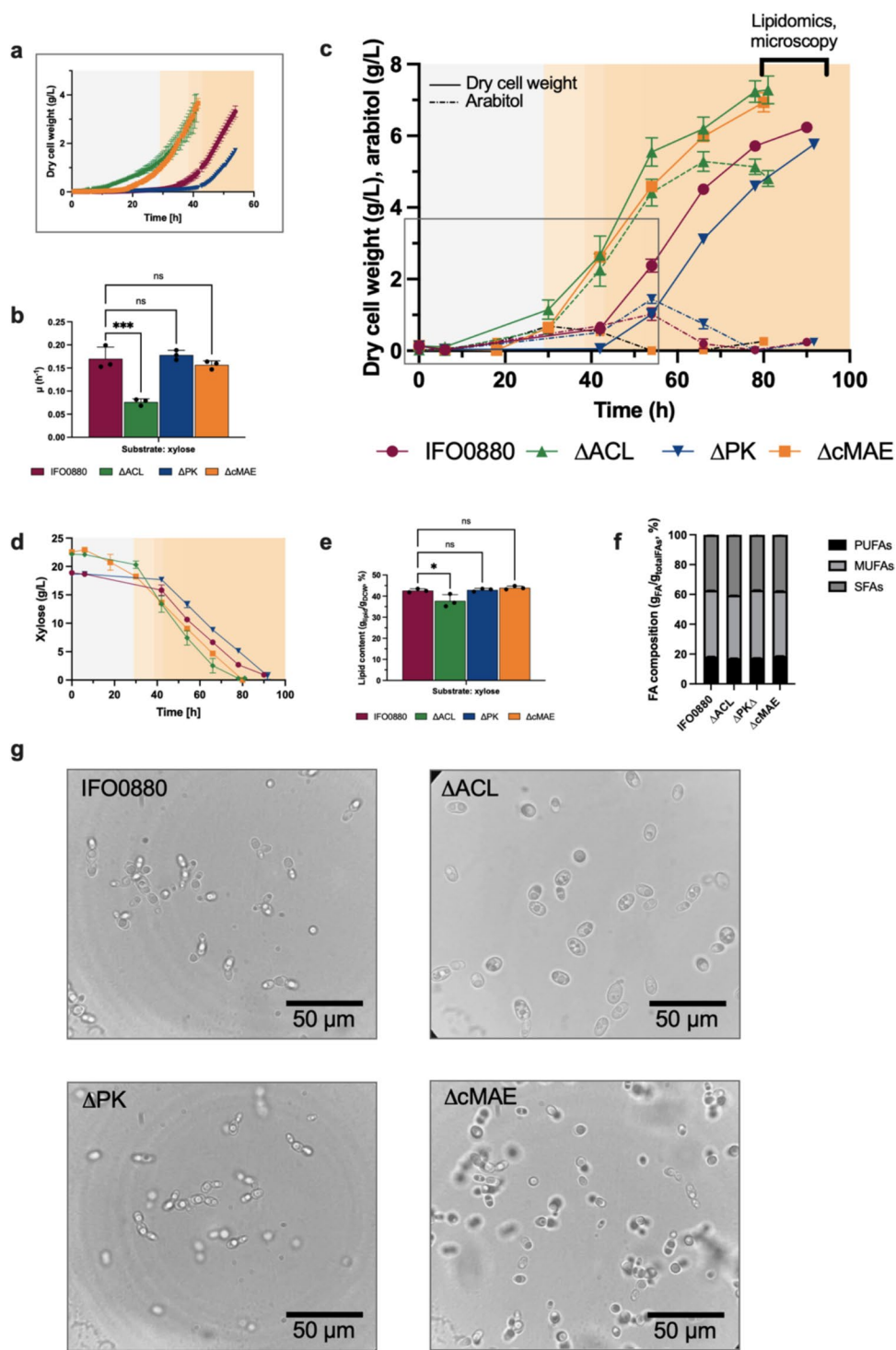
The fatty acid composition of the wild type *R. toruloides* IFO0880 was C16:0 22.67% and C18:1 45.62% (g<sub>FA</sub>/g<sub>totalFA</sub>) (Table 3), closely similar to as previously reported (Ratledge and Wynn 2002). In fact, our results were closely similar to the *R. glutinis* strain, which has more recently been designated as *R. toruloides*, and according to Zhang et al. may even be IFO0880 (Zhang et al. 2016b). The knockout of the ACL caused changes in the fatty acid composition. We observed a relative increase in polyunsaturated fatty acids (C18:2 and C18:3) of 34% of total fatty acids when compared to the wild type strain (g<sub>FA</sub>/g<sub>totalFA</sub>) (Fig. 2f). In the ACL knockout, the fraction of oleic acid (C18:1) decreased significantly compared to the wild type strain and constituted only 19.47% (*p*val < 0.0001), while linoleic acid (C18:2) increased significantly compared to the wild type and became the largest fraction with 29.46% (*p*val < 0.0001), followed by 17.78% of alpha-linoleic acid (C18:3) (Table 3, *p*val < 0.0001). Similar observations were reported in *Y. lipolytica* (Dulermo et al. 2015). It should be noted, however, that when calculated per DCW, the total quantities of all measured fractions decreased compared to the wild type strain (Supplementary Table S3).

Yeasts and filamentous fungi undergo morphological differentiations when triggered by extracellular stimuli such as nutrient limitation. Therefore, we examined cells harvested at the end of the experiment under the microscope. We observed that the majority of strains, including the wild type, had adopted linear chain morphology (Fig. 2g), notably different from their typical oval-shaped unicellular form (Supplementary Fig. S4). Similar morphological appearance, also known as pseudohyphae formation, has been observed at slow growth rates below 0.1 h<sup>-1</sup> in glucose-limited chemostats of the non-conventional yeast *Komagataella phaffii* (Rebnegger et al. 2014) and *S. cerevisiae* under the nitrogen limitation (Gimeno et al. 1992). However, as a result

**Table 3** Bioreactor data and fatty acid composition (g<sub>FA</sub>/g<sub>totalFA</sub>, %) measured by GC-FID for strains grown in the glucose-based (20 g/L) pH-adjusted chemically defined low-nitrogen medium (C/N of 80). C16:0 palmitic acid, C18:0 stearic acid, C18:1(c9) oleic acid,

C18:2(n6) linoleic acid, C18:3(n3) alpha-linolenic acid, and FAs fatty acids. Mean and standard deviation are calculated from three biological replicates

Strain	Dry cell weight (g/L)	Lipid content (g <sub>lipid</sub> /g <sub>DCW</sub> , %)	Major fatty acid residues (g <sub>FA</sub> /g <sub>totalFAs</sub> , %)						Harvest time (h)
			C16:0	C18:0	C18:1(c9)	C18:2(n6)	C18:3(n3)	Other FAs	
IFO0880 (NBRC 0880)	10.23 ± 0.15	50.18 ± 0.37	22.67 ± 0.14	12.62 ± 0.06	45.62 ± 0.11	11.38 ± 0.14	3.58 ± 0.01	4.13	54
ΔPK	10.23 ± 0.15	50.52 ± 0.94	22.70 ± 0.10	12.64 ± 0.12	45.73 ± 0.14	11.29 ± 0.06	3.50 ± 0.01	4.14	54
ΔACL	2.34 ± 0.065	9.43 ± 0.039	16.25 ± 0.03	9.42 ± 0.09	19.47 ± 0.49	29.46 ± 0.28	17.78 ± 0.16	7.61	54
ΔcMAE	9.62 ± 0.26	51.64 ± 0.50	22.80 ± 0.10	11.72 ± 0.07	46.04 ± 0.12	11.49 ± 0.12	3.90 ± 0.06	4.04	48



of the knockout of the ACL gene, cells did not form these filament-like structures (Fig. 2g), instead their morphology looked very similar to that during the exponential growth phase (Supplementary Fig. S4), in a good agreement with the above analysis that the loss of ACL indeed deprived cells from consuming carbon under nitrogen limitation.

### Xylose as a carbon source modifies the cellular response to ACL loss

*R. toruloides* can consume xylose as a sole carbon source (Pinheiro et al. 2020). DCW of 18 (g/L) on xylose as a carbon source was comparable to the one grown on glucose, 22 (g/L), but the DCW yield on substrate ( $g_{\text{DCW}}/g_{\text{substrate}}$ ) even

**Fig. 3** Physiological parameters obtained in xylose-based pH-adjusted low-nitrogen mineral medium (C/N ratio 80) (Verduyn et al. 1992). Data obtained from cultivating *R. toruloides* wild type IFO0880 (circle), ATP citrate lyase knockout ( $\Delta$ ACL, pyramid), phosphoketolase knockout ( $\Delta$ PK, inverted pyramid), and cytosolic malic enzyme knockout ( $\Delta$ cMAE, square) strains in falcon tube bioreactors with non-invasive OD, dO<sub>2</sub>, and pH sensors. **a** A snapshot of the online OD<sub>600</sub> data displayed as the dry cell weight (g/L), **b** maximum specific growth rate fitted from the exponential growth phase OD<sub>600</sub> data (h<sup>-1</sup>), **c** dry cell weight and arabitol (g/L), **d** substrate concentration (g/L), **e** lipid content (g<sub>lipid</sub>/g<sub>DCW</sub>, %); cells harvested at the end of cultivation, **f** relative fatty acid composition (g<sub>FA</sub>/g<sub>totalFAs</sub>, %); cells harvested at the end of cultivation, **g** morphology comparison of wild type IFO0880 versus knockout strains visualized by bright-field microscope; cells harvested at the end of cultivation. Panels **a** and **c** background colors denote the switch in growth phases based on dO<sub>2</sub> curves available from Supplementary Fig. S2, presumably pointing to the onset of the nitrogen limitation phase. FAs fatty acids, SFAs saturated fatty acids, MUFA monounsaturated fatty acids, PUFA polyunsaturated fatty acids. Error bars are calculated as a standard deviation from three biological experiments. Asterisks denote statistical significance (ANOVA Dunnett's multiple comparison test against the wild type IFO0880 strain, adjusted *p* value \**p*<0.05, \*\**p*<0.01, \*\*\**p*<0.001, \*\*\*\**p*<0.0001). ns is used to denote changes that are statistically nonsignificant

outperformed glucose (Pinheiro et al. 2020). Xylose is a relevant substrate of *R. toruloides* that has been less explored; therefore, we cultivated  $\Delta$ PK,  $\Delta$ ACL, and  $\Delta$ cMAE strains in the low-nitrogen pH-adjusted chemically defined medium, but this time containing xylose as a sole carbon source. All strains demonstrated slightly different lag phases, but the ACL knockout exhibited the shortest lag phase and the lowest specific growth rate compared to the wild type strain (Fig. 3a, Supplementary Table S2). The specific growth rate ( $\mu$ ) was 45% of the wild type strain (Fig. 3b, apval<0.001). Nevertheless, ACL knockout reached even a significantly higher final DCW titer as compared to the wild type strain (Fig. 3c, Supplementary Fig. S3, b, apval<0.01) and consumed xylose until depletion (Fig. 3d). The non-lipid DCW

titors of the ACL knockout were higher compared to the wild type strain (apval<0.01), suggesting that ACL was involved in other cellular processes apart from lipid synthesis (Supplementary Fig. S3b). Lipid content of the wild type strain was  $42.61 \pm 0.84\%$  (g<sub>lipid</sub>/g<sub>DCW</sub>) after 90 h of growth on low-nitrogen mineral medium (Table 4), but the ACL knockout gave significantly lower,  $37.71 \pm 3.01\%$  (g<sub>lipid</sub>/g<sub>DCW</sub>) (Fig. 3e, apval 0.02), with no major changes in the fatty acid profiles (Fig. 3f, Table 4). Linear chain pseudohyphal growth was unchanged compared to the glucose medium. Chain-like pseudohyphal growth was observed for all strains, except for the ACL knockout (Fig. 3g). The knockout of the cMAE gene did not have an effect on growth or lipid synthesis on medium containing xylose as a carbon source (Fig. 3a–f).

Altogether, these results indicated that *R. toruloides* IFO0880 is less reliant on ACL than assumed, which suggests an alternative source of cytosolic acetyl-CoA on xylose as sole carbon source. It cannot be ruled out that the PK replaced ACL for the supply of acetyl-CoA upon the ACL knockout, but on the other hand, the knockout of the PK gene alone did not give any change in the specific growth rate or lipid content (Fig. 3a–f). We speculate that one of the options for the cytosolic acetyl-CoA synthesis could be the pyruvate-acetaldehyde-acetate pathway, also known as “pyruvate dehydrogenase bypass.” Despite low protein expression levels of ACS on glucose and xylose, it was previously reported higher abundant on xylose during the exponential growth (*p* value 0.038) and lipid accumulation phase (*p* value 0.49) compared to glucose-grown cells (Rekēna et al. 2023).

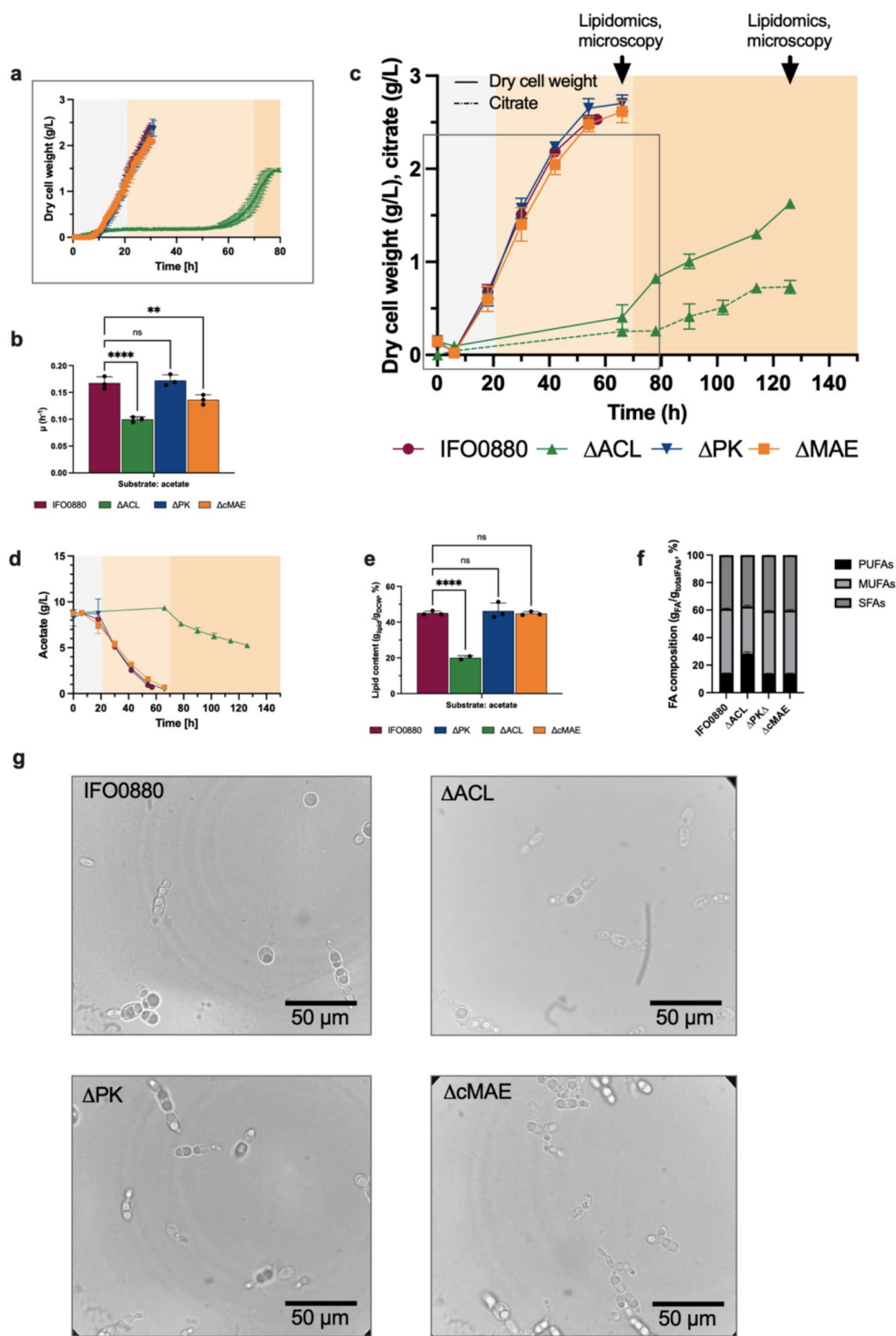
#### ACL loss demonstrates negative effects on cell growth and lipid synthesis on acetate

Previous reports have shown differences in growth response on acetate caused by loss of ACL. In pathogenic

**Table 4** Bioreactor data and fatty acid composition (g<sub>FA</sub>/g<sub>totalFAs</sub>, %) measured by GC-FID for strains grown in the xylose-based (20 g/L) pH-adjusted chemically defined low-nitrogen medium (C/N of 80). C16:0 palmitic acid, C18:0 stearic acid, C18:1(c9) oleic acid,

C18:2(n6) linoleic acid, C18:3(n3) alpha-linolenic acid, FAs fatty acids. Mean and standard deviation are calculated from three biological replicates

Strain	Dry cell weight (g/L)	Lipid content (g <sub>lipid</sub> /g <sub>DCW</sub> , %)	Major fatty acid residues (g <sub>FA</sub> /g <sub>totalFAs</sub> , %)						Harvest time (h)
			C16:0	C18:0	C18:1(c9)	C18:2(n6)	C18:3(n3)	Other FAs	
IFO0880 (NBRC 0880)	$6.24 \pm 0.13$	$42.61 \pm 0.84$	$21.80 \pm 0.03$	$11.42 \pm 0.03$	$43.52 \pm 0.06$	$14.65 \pm 0.17$	$3.30 \pm 0.03$	5.31	90
$\Delta$ PK	$5.76 \pm 0.075$	$42.94 \pm 0.73$	$21.28 \pm 0.19$	$11.61 \pm 0.19$	$44.44 \pm 0.24$	$13.70 \pm 0.11$	$3.40 \pm 0.03$	5.57	91
$\Delta$ ACL	$7.28 \pm 0.39$	$37.71 \pm 3.01$	$28.27 \pm 0.09$	$9.47 \pm 0.16$	$41.05 \pm 0.05$	$14.67 \pm 0.18$	$2.18 \pm 0.07$	4.35	81
$\Delta$ cMAE	$6.93 \pm 0.27$	$43.94 \pm 0.82$	$22.21 \pm 0.11$	$11.36 \pm 0.06$	$42.62 \pm 0.15$	$14.85 \pm 0.18$	$3.51 \pm 0.02$	5.45	80



basidiomycetous yeast *C. neoformans*, the knockout of the ACL1 gene caused growth defects on glucose, but no effect during growth on acetate (Griffiths et al. 2012). In oleaginous ascomycetous yeast *L. starkeyi*, a knockout of both ACL1 and ACL2 gene resulted in restored growth on acetate, but TAG productivity was lower than that of the control using acetate with glucose (Sato et al. 2021). In

accordance with these reports, we cultivated ΔPK, ΔACL, ΔcMAE strains, and IFO0880 in low-nitrogen chemically defined medium with acetate as a sole carbon source. The initial medium pH was adjusted to 6 by adding KOH and was not maintained. During the cultivation, the pH in all cultures rose equally, as the cells started growing, and reached pH 9 at the end of cultivation (Supplementary

**Fig. 4** Physiological parameters obtained in acetate-based pH 7-adjusted low-nitrogen mineral medium (C/N ratio 80) (Verduyn et al. 1992). Data obtained from cultivating *R. toruloides* wild type IFO0880 (circle), ATP citrate lyase knockout ( $\Delta$ ACL, pyramid), phosphoketolase knockout ( $\Delta$ PK, inverted pyramid), and cytosolic malic enzyme knockout ( $\Delta$ cMAE, square) strains in falcon tube bio-reactors with non-invasive OD, dO<sub>2</sub>, and pH sensors. **a** A snapshot of the online OD<sub>600</sub> data displayed as the dry cell weight (g/L), **b** maximum specific growth rate fitted from the exponential growth phase OD<sub>600</sub> data (h<sup>-1</sup>), **c** dry cell weight and citrate (g/L), **d** substrate concentration (g/L), **e** lipid content (g<sub>lipid</sub>/g<sub>DCW</sub>, %); cells harvested at the end of cultivation, **f** relative fatty acid composition (g<sub>FA</sub>/g<sub>totalFA</sub>, %); cells harvested at the end of cultivation, **g** morphology comparison of wild type IFO0880 versus knockout strains visualized by bright-field microscope; cells harvested at the end of cultivation. Panels **a** and **c** background colors denote the switch in growth phases based on dO<sub>2</sub> curves available from Supplementary Fig. S2, presumably pointing to the onset of the nitrogen limitation phase. FAs fatty acids, SFAs saturated fatty acids, MUFA monounsaturated fatty acids, PUFA polyunsaturated fatty acids. Error bars are calculated as a standard deviation from three biological experiments. Asterisks denote statistical significance (ANOVA Dunnett's multiple comparison test against the wild type IFO0880 strain, adjusted *p* value \**p*<0.05, \*\**p*<0.01, \*\*\**p*<0.001, \*\*\*\**p*<0.0001). ns is used to denote changes that are statistically nonsignificant

Fig. S1). The growth of  $\Delta$ ACL was extremely delayed as compared to the other strains (Fig. 4a), and the maximum specific growth rate was reduced by 40% in comparison to wild type strain (Fig. 4b, apval 0.009), falling to  $0.10 \pm 0.0047$  h<sup>-1</sup> (Supplementary Table S2). The ACL knockout started growing only at 60 h and 6 h after that started to produce slight amounts of citrate, a substrate for ACL (Fig. 4c). Although the analysis showed a consistent, slow consumption of acetate after 66 h,  $\Delta$ ACL cells stopped respiring before all the acetate was depleted around 126 h (Fig. 4d, Supplementary Fig. S1). Other strains consumed the substrate completely with no visible disturbance to the growth rates. These results demonstrated that *R. toruloides* responded similarly to ACL loss compared to glucose medium, and acetate did not restore the growth defects caused by ACL loss. It was in contrast to findings by Hynes and Murray, in which the authors concluded that external sources of cytoplasmic acetyl-CoA result in repression of ACL (Hynes and Murray 2010). The loss of ACL caused 56% reduction in lipids (g<sub>lipid</sub>/g<sub>DCW</sub>) (Fig. 4e, apval < 0.0001) and alterations in fatty acid profiles (Fig. 4f). On acetate, ACL loss did not result in significant changes to non-lipid DCW (Supplementary Fig. S3c), indicating that the effect was directly on lipid synthesis and not beyond as in case of the glucose-grown cells. The majority fatty acid fraction, C18:1, decreased relatively from 46 to 33% (g<sub>FA</sub>/g<sub>totalFA</sub>), while C18:2 and C18:3 increased relatively to 20% and 8%, respectively, 20% of C18:2 and 8% of C18:3 (g<sub>FA</sub>/g<sub>totalFA</sub>) (Table 5). These results were similar to the *L. starkeyi* study, in which the TAG productivity of the ACL knockout

strain was significantly lower compared to the reference strain on medium containing glucose and acetate (Sato et al. 2021). It also indicated that acetate must be converted into citrate for its assimilation, which is possible if mitochondrial malate-oxoglutarate and oxoglutarate/citrate shuttling takes place.

cMAE knockout gave a 19% decrease in the specific growth rate, falling to  $0.14 \pm 0.0091$  h<sup>-1</sup> (apval 0.009), even though it did not affect the lipid content (Table 5). These results suggested that cMAE is not involved in lipogenesis on acetate. Consistent with the above results, the knockout of the PK gene caused no change in growth or lipid synthesis (Fig. 4a-f).

Growth on acetate induced differences in cell morphology in this experiment. Cells formed less chain-like structures compared to glucose or xylose-grown cells, even though they were under nutrient starvation (Fig. 4g).

## Discussion

*R. toruloides* is an emerging oleaginous cell factory for the production of fats, oils, and oleochemicals. The metabolic mechanisms of lipid production in *R. toruloides* are less understood compared to other oleaginous fungi *M. circinelloides* or *M. alpina*, oleaginous yeast *Y. lipolytica*, or model yeast *S. cerevisiae*. Due to the development of gene editing tools (Otoupal et al. 2019; Liu et al. 2019; Jiao et al. 2019; Schultz et al. 2019), the possibilities for functional genomics studies are significantly improved. In this study, we applied CRISPR/Cas9 genome editing system to elucidate the role of PK pathway, ACL, and cMAE in lipid biosynthesis of *R. toruloides* IFO0880 by creating gene knockouts and characterizing them on alternative carbon sources.

The results of this study demonstrated that ACL is crucial for not only the fatty acid synthesis but also for growth in *R. toruloides*. Loss of ACL reduced lipid content by 81% of DCW compared to the wild type strain on glucose, 11% on xylose and 56% on acetate (Figs. 2, 3, and 4). It also significantly reduced the specific growth rate on all carbon sources. Although previous studies have reported growth defects as a result of ACL inactivation in *A. niger*, *A. nidulans*, *S. macrospora*, and *Y. lipolytica* (Nowrousian et al. 1999; Hynes and Murray 2010; Chen et al. 2014; Dulermo et al. 2015), the present study revealed a difference to *Y. lipolytica*. ACL knockout resulted in a growth arrest on glucose and on acetate once nitrogen is depleted, as demonstrated by a significantly lower cell density compared to the reference strain by the end of experiment (see Figs. 2 and 4). On glucose, it could not have been caused by the pH changes, because it remained within the optimal range (pH 5.5–7.0) throughout cultivation (Supplementary Fig. S1). Currently, there is not enough evidence to provide a single explanation

**Table 5** Bioreactor data and fatty acid composition ( $g_{FA}/g_{totalFAs}$ , %) measured by GC-FID for strains grown in the acetate-based (20 g/L) chemically defined low-nitrogen medium (C/N of 80). C16:0 palmitic

Strain	Dry cell weight (g/L)	Lipid content ( $g_{lipid}/g_{DCW}$ , %)	Major fatty acid residues ( $g_{FA}/g_{totalFAs}$ , %)							Harvest time (h)
			C16:0	C18:0	C18:1(c9)	C18:2(n6)	C18:3(n3)	Other FAs		
IFO0880 (NBRC 0880)	2.53 ± 0.03	45.07 ± 1.15	17.30 ± 0.26	18.35 ± 0.12	46.04 ± 0.31	9.83 ± 0.02	4.07 ± 0.08	4.41	54	
ΔPK	2.70 ± 0.09	46.23 ± 4.45	18.53 ± 0.37	18.64 ± 0.19	44.81 ± 0.47	9.40 ± 0.13	4.14 ± 0.09	4.48	66	
ΔACL	1.63 ± 0.03	20.02 ± 1.18	17.27 ± 0.04	15.69 ± 0.37	33.06 ± 0.91	19.69 ± 0.83	8.10 ± 0.39	6.21	66	
ΔcMAE	2.62 ± 0.12	44.79 ± 1.05	18.25 ± 0.45	18.48 ± 0.07	45.09 ± 0.65	9.49 ± 0.04	4.19 ± 0.07	4.49	126	

to our observations. Lowered acetyl-CoA in cytoplasm impairs the synthesis of signaling molecules and secondary metabolites leading to developmental effects (Hynes and Murray 2010). In yeast, acetyl-CoA is localized in four different compartments, and nuclear acetyl-CoA is required for histone acetylation (Takahashi et al. 2006; Pietrocola et al. 2015). Recently, the role of ACL in supplying acetyl-CoA for histone acetylation to promote proliferation was demonstrated in myeloid cells (Rhee et al. 2019). Another consequence of the ACL knockout is likely impaired citrate conversion to cytosolic acetyl CoA that probably leads to citrate oxidation in mitochondria and an increased flux through the TCA cycle increasing the production of substrates for the electron transport chain, which was confirmed by proving elevated mitochondrial membrane potential between control and ACL knockdown cells in hematopoietic murine cells (Board and Newsholme 1996; Bauer et al. 2005). It is in line with the detected extracellular citrate on acetate (Fig. 4c). In this study, we also observed an effect on cell morphology during nitrogen limitation. In *S. cerevisiae*, it has been investigated that pseudohyphal growth is regulated by two different signaling pathways, the MAP kinase cascade and cAMP-dependent pathway (Gancedo 2001). In mammalian cells, ACL is hierarchically regulated through cAMP-dependent phosphorylation (Pierce et al. 1981; Pant et al. 2023). The observed morphological changes, growth arrest during nitrogen starvation, and the drop in lipid production that were all associated with the ACL loss suggest a complex regulatory network regulation of ACL in *R. toruloides*. The comparison of lipid content to ACL loss in glucose, xylose, and acetate media indicated very interesting carbon-source dependent differences in metabolic regulation and the existence of alternative routes to cytosolic acetyl-CoA. To our best knowledge, this is the first report characterizing ACL knockout in yeast in the xylose medium. While these results are more in agreement with what was reported earlier in *Y. lipolytica* on glucose, further studies are required to understand why in *R. toruloides* the knockout responses on xylose

acid, C18:0 stearic acid, C18:1(c9) oleic acid, C18:2(n6) linoleic acid, C18:3(n3) alpha-linolenic acid, and FAs fatty acids. Mean and standard deviation are calculated from three biological replicates

and glucose were different. On a preliminary level, we speculated that upon knockout of ACL on xylose, the acetyl-CoA synthetase (ACS) could be used for the synthesis of cytosolic acetyl-CoA resulting in higher lipid content, while in glucose and acetate media the main role was staying with the ACL. It is known that ACS is transcriptionally regulated (Chen et al. 2012) and the only source of cytosolic acetyl-CoA (Pronk et al. 1996) in *S. cerevisiae*. Large differences in signaling pathways under the consumption of xylose have already been reported, but mainly in *S. cerevisiae*. Assimilation of xylose is weakly sensed by the intracellular branch of the cAMP/PKA pathway in yeast (Brink et al. 2021).

In this study, we showed that the lipid production was not changed as a result of the PK knockout (Figs. 2, 3, and 4). Unintuitively, our result also did not support the evidence from early biochemical studies on xylose as a carbon source. Compared to the alternative biosynthetic pathways for cytosolic acetyl-CoA production, the PK route bypasses the decarboxylation step of pyruvate into CO<sub>2</sub> and acetaldehyde (catalyzed by pyruvate decarboxylase) and the ATP expenditure for the activation of acetate by ACS or citrate by ACL, thus potentially increasing the acetyl-CoA yield. We thought it was the reason why previously stoichiometric genome-scale modeling predicted the PK route for the utilization of glucose or xylose in *R. toruloides* (Lopes et al. 2020; Rečena et al. 2023) being in the agreement with previous enzyme abundance studies (Kim et al. 2021; Rečena et al. 2023). But our results did not support this hypothesis on either of the substrates. Based on existing genetic engineering studies, we speculated that the metabolic flux can be rerouted through PK in a combination with silencing the expression of other enzymes in a close proximity. In *Y. lipolytica*, expression of PK worked to improve lipid production in phosphofructokinase (PFK) deletion background (Kamineni et al. 2021). Introduction of PK pathway was demonstrated in TKT and TAL deletion background to produce 3HP in *S. cerevisiae* (Hellgren et al. 2020). On the other hand, *R. toruloides* PK K<sub>m</sub> value would potentially explain why the PK is not critical

for lipid synthesis in the wild type strain. Alternatively, the bottleneck could be PTA or acetate kinase (ACK). Overexpression of non-native PTA improved lipid titers in *R. toruloides* NP11 by 15.1% (Yang et al. 2018), but the role of ACK in *R. toruloides* still needs to be studied. In non-oleaginous *A. niger*, which has a native PK pathway, heterologous PK pathway expression increased target product synthesis, while the deletion of ACK decreased it (Liu et al. 2023). Also, it is worth noting that in the enzyme database BRENDa, the PTA reaction equation denotes acetyl-CoA as a substrate and acetyl-phosphate as a product. The thermodynamic feasibility of the pathway is unclear.

Finally, the results of this study suggested that cMAE plays no significant role in lipogenesis in *R. toruloides* IFO0880 and its presence has an adverse effect when growing on glucose. It was in good agreement with the early biochemical studies with *R. glutinis* (Yoon et al. 1984). Compared to the catabolic pathways of glucose or xylose, acetate assimilation requires less enzymatic conversions to synthesize the substrate of malic enzyme and, perhaps, the reason why stoichiometric genome-scale models have predicted the use of cMAE for NADPH regeneration upon assimilation of acetate (Lopes et al. 2020; Rekēna et al. 2023). Our results confirmed that cytosolic malic enzyme is not critical for lipogenesis, suggesting that alternative routes for NADPH regeneration can be used, likely enzymes from the oxidative pentose phosphate pathway. Recent genetic engineering studies are available only on glucose. Lipogenesis induction upon a knockout was reported by Dulermo et al., when a mMae in *Y. lipolytica* was deleted (Dulermo et al. 2015); although *Y. lipolytica* does not have a cMAE. Nevertheless, there is a slight difference that in wild type background, such an effect was not observed, but in an engineered strain for lipid production (“Obese”), the adverse effect was observed. Perhaps we can say that according to our evidence, a wild type background is an even stronger argument for the cMAE non-essentiality in lipogenesis. But it is worth noting that overexpression of native cMAE in *R. toruloides* IFO0880 (same strain) increased lipid titers by 28% (Zhang et al. 2016a). Authors noted that this was a relatively minor increase compared to other enzymes that were introduced, but it shows that cMAE can play a role in lipogenesis of *R. toruloides* under certain conditions (e.g., overexpression).

In conclusion, we showed that ACL is essential for lipid synthesis and cell growth in *R. toruloides*. The cellular response to ACL loss was affected by the carbon source present in cultivation media. The results also demonstrated that cytosolic malic enzyme is not critically involved in lipid synthesis in *R. toruloides* and in some conditions is even disfavorable. The characterization of the PK knockout suggested that it is not critical for the lipid synthesis. This work

is useful for future metabolic engineering strategies of *R. toruloides*.

**Supplementary Information** The online version contains supplementary material available at <https://doi.org/10.1007/s00253-025-13454-w>.

**Acknowledgements** We thank Dr. Peter Otoopal for providing us the pPBO.202 plasmid. We also acknowledge Olesia Duda for the fatty acid analysis.

**Author contribution** AR and PJL conceptualized and designed the study. AR and KP conducted experiments. SG contributed to genetic engineering methodology. AR analyzed data and wrote the manuscript. All authors read and approved the manuscript.

**Funding** This study was funded by the Estonian Research Council Grant PRG1011 and European Union’s HORIZON Teaming for Excellence program under grant agreement 101060066.

**Data availability** The authors declare that the data supporting the findings of this study are available within the paper and its Supplementary Information files.

## Declarations

**Competing interests** The authors declare no competing interests.

**Open Access** This article is licensed under a Creative Commons Attribution-NonCommercial-NoDerivatives 4.0 International License, which permits any non-commercial use, sharing, distribution and reproduction in any medium or format, as long as you give appropriate credit to the original author(s) and the source, provide a link to the Creative Commons licence, and indicate if you modified the licensed material. You do not have permission under this licence to share adapted material derived from this article or parts of it. The images or other third party material in this article are included in the article’s Creative Commons licence, unless indicated otherwise in a credit line to the material. If material is not included in the article’s Creative Commons licence and your intended use is not permitted by statutory regulation or exceeds the permitted use, you will need to obtain permission directly from the copyright holder. To view a copy of this licence, visit <http://creativecommons.org/licenses/by-nc-nd/4.0/>.

## References

- Ageitos JM, Vallejo JA, Veiga-Crespo P, Villa TG (2011) Oily yeasts as oleaginous cell factories. *Appl Microbiol Biotechnol* 90:1219–1227. <https://doi.org/10.1007/s00253-011-3200-z>
- Bauer DE, Hatzivassiliou G, Zhao F, Andreadis C, Thompson CB (2005) ATP citrate lyase is an important component of cell growth and transformation. *Oncogene* 24:6314–6322. <https://doi.org/10.1038/sj.onc.1208773>
- Beopoulos A, Nicaud J-M, Gaillardin C (2011) An overview of lipid metabolism in yeasts and its impact on biotechnological processes. *Appl Microbiol Biotechnol* 90:1193–1206. <https://doi.org/10.1007/s00253-011-3212-8>
- Blazeck J, Hill A, Liu L, Knight R, Miller J, Pan A, Otoopal P, Alper HS (2014) Harnessing *Yarrowia lipolytica* lipogenesis to create a platform for lipid and biofuel production. *Nat Commun* 5:3131. <https://doi.org/10.1038/ncomms4131>

- Board M, Newsholme E (1996) Hydroxycitrate causes altered pyruvate metabolism by tumorigenic cells. *IUBMB Life* 40:1047–1056. <https://doi.org/10.1080/15216549600201683>
- Bonturi N, Pinheiro MJ, De Oliveira PM, Rusadze E, Eichinger T, Liudžiūtė G, De Biaggi JS, Brauer A, Remm M, Miranda EA, Ledesma-Amaro R, Lahtvee P-J (2022) Development of a dedicated Golden Gate Assembly Platform (RtGGA) for *Rhodotorula toruloides*. *Metab Eng Commun* 15:e00200. <https://doi.org/10.1016/j.mec.2022.e00200>
- Botham PA, Ratledge C (1979) A biochemical explanation for lipid accumulation in *Candida* 107 and other oleaginous microorganisms. *J Gen Microbiol* 114:361–375. <https://doi.org/10.1099/00221287-114-2-361>
- Boulton CA, Ratledge C (1981) Correlation of lipid accumulation in yeasts with possession of ATP: citrate lyase. *Microbiology* 127:169–176. <https://doi.org/10.1099/00221287-127-1-169>
- Brink DP, Borgström C, Persson VC, Ofuji Osiro K, Gorwa-Grauslund MF (2021) D-xylose sensing in *Saccharomyces cerevisiae*: insights from D-glucose signaling and native D-xylose utilizers. *Int J Mol Sci* 22:12410. <https://doi.org/10.3390/ijms22212410>
- Cao M, Tran VG, Qin J, Olson A, Mishra S, Schultz JC, Huang C, Xie D, Zhao H (2022) Metabolic engineering of oleaginous yeast *Rhodotorula toruloides* for overproduction of triacetic acid lactone. *Biotechnol Bioeng* 119:2529–2540. <https://doi.org/10.1002/bit.28159>
- Chattopadhyay A, Mitra M, Maiti MK (2021) Recent advances in lipid metabolic engineering of oleaginous yeasts. *Biotechnol Adv* 53:107722. <https://doi.org/10.1016/j.biotechadv.2021.107722>
- Chawla K, Kaur S, Kaur R, Bhunia RK (2022) Metabolic engineering of oleaginous yeasts to enhance single cell oil production. *J Food Process Eng* 45:e13634. <https://doi.org/10.1111/jfpe.13634>
- Chen Y, Siewers V, Nielsen J (2012) Profiling of cytosolic and peroxisomal acetyl-CoA metabolism in *Saccharomyces cerevisiae*. *PLoS ONE* 7:e42475. <https://doi.org/10.1371/journal.pone.0042475>
- Chen H, He X, Geng H, Liu H (2014) Physiological characterization of ATP-citrate lyase in *Aspergillus niger*. *J Ind Microbiol Biotechnol* 41:721–731. <https://doi.org/10.1007/s10295-014-1418-3>
- Coradetti ST, Pinel D, Geiselman GM, Ito M, Mondo SJ, Reilly MC, Cheng Y-F, Bauer S, Grigoriev IV, Gladden JM, Simmons BA, Brem RB, Arkin AP, Skerker JM (2018) Functional genomics of lipid metabolism in the oleaginous yeast *Rhodosporidium toruloides*. *eLife* 7:e32110. <https://doi.org/10.7554/eLife.32110>
- Dinh HV, Suthers PF, Chan SHJ, Shen Y, Xiao T, Deewan A, Jagtap SS, Zhao H, Rao CV, Rabinowitz JD, Maranas CD (2019) A comprehensive genome-scale model for *Rhodosporidium toruloides* IFO0880 accounting for functional genomics and phenotypic data. *Metab Eng Commun* 9:e00101. <https://doi.org/10.1016/j.mec.2019.e00101>
- Donzella S, Cucchetti D, Capusoni C, Rizzi A, Galafassi S, Chiara G, Compagno C (2019) Engineering cytoplasmic acetyl-CoA synthesis decouples lipid production from nitrogen starvation in the oleaginous yeast *Rhodosporidium azoricum*. *Microb Cell Factories* 18:199. <https://doi.org/10.1186/s12934-019-1250-6>
- Dourou M, Aggelis D, Papanikolaou S, Aggelis G (2018) Critical steps in carbon metabolism affecting lipid accumulation and their regulation in oleaginous microorganisms. *Appl Microbiol Biotechnol* 102:2509–2523. <https://doi.org/10.1007/s00253-018-8813-z>
- Dulermo T, Lazar Z, Dulermo R, Rakicka M, Haddouche R, Nicaud J-M (2015) Analysis of ATP-citrate lyase and malic enzyme mutants of *Yarrowia lipolytica* points out the importance of mannitol metabolism in fatty acid synthesis. *Biochim Biophys Acta BBA - Mol Cell Biol Lipids* 1851:1107–1117. <https://doi.org/10.1016/j.bbalip.2015.04.007>
- Evans CT, Ratledge C (1984) Induction of xylulose-5-phosphate phosphotolase in a variety of yeasts grown on d-xylose: the key to efficient xylose metabolism. *Arch Microbiol* 139:48–52. <https://doi.org/10.1007/BF00692711>
- Fatland BL, Ke J, Anderson MD, Mentzen WI, Cui LW, Allred CC, Johnston JL, Nikolau BJ, Wurtele ES (2002) Molecular characterization of a heteromeric ATP-citrate lyase that generates cytosolic acetyl-coenzyme a in arabidopsis. *Plant Physiol* 130:740–756. <https://doi.org/10.1104/pp.008110>
- Gancedo JM (2001) Control of pseudohyphae formation in *Saccharomyces cerevisiae*. *FEMS Microbiol Rev* 25:107–123. <https://doi.org/10.1111/j.1574-6976.2001.tb00573.x>
- Gimeno CJ, Ljungdahl PO, Styles CA, Fink GR (1992) Unipolar cell divisions in the yeast *S. cerevisiae* lead to filamentous growth: regulation by starvation and RAS. *Cell* 68:1077–1090. [https://doi.org/10.1016/0092-8674\(92\)90079-R](https://doi.org/10.1016/0092-8674(92)90079-R)
- Gong G, Wu B, Liu L, Li J, He M (2024) Engineering oleaginous red yeasts as versatile chassis for the production of olechemicals and valuable compounds: current advances and perspectives. *Bio-technol Adv* 108432. <https://doi.org/10.1016/j.biotechadv.2024.108432>
- Griffiths EJ, Hu G, Fries B, Caza M, Wang J, Gsponer J, Gates-Hollingsworth MA, Kozel TR, De Repentigny L, Kronstad JW (2012) A defect in ATP-citrate lyase links acetyl-CoA production, virulence factor elaboration and virulence in *Cryptococcus neoformans*. *Mol Microbiol* 86:1404–1423. <https://doi.org/10.1111/mmi.12065>
- Hellgren J, Godina A, Nielsen J, Siewers V (2020) Promiscuous phosphotolase and metabolic rewiring enables novel non-oxidative glycolysis in yeast for high-yield production of acetyl-CoA derived products. *Metab Eng* 62:150–160. <https://doi.org/10.1016/j.ymben.2020.09.003>
- Hynes MJ, Murray SL (2010) ATP-citrate lyase is required for production of cytosolic acetyl coenzyme A and development in *Aspergillus nidulans*. *Eukaryot Cell* 9:1039–1048. <https://doi.org/10.1128/EC.00080-10>
- Jiao X, Zhang Y, Liu X, Zhang Q, Zhang S, Zhao ZK (2019) Developing a CRISPR/Cas9 system for genome editing in the basidiomycetous yeast *Rhodosporidium toruloides*. *Biotechnol J* 14:1900036. <https://doi.org/10.1002/biot.201900036>
- Jinek M, Chylinski K, Fonfara I, Hauer M, Doudna JA, Charpentier E (2012) A programmable dual-RNA-guided DNA endonuclease in adaptive bacterial immunity. *Science* 337:816–821. <https://doi.org/10.1126/science.1225829>
- Kamineni A, Consiglio AL, MacEwen K, Chen S, Chifamba G, Shaw AJ, Tsakraklides V (2021) Increasing lipid yield in *Yarrowia lipolytica* through phosphotolase and phosphotransacetylase expression in a phosphofructokinase deletion strain. *Biotechnol Biofuels* 14:113. <https://doi.org/10.1186/s13068-021-01962-6>
- Kim J, Coradetti ST, Kim Y-M, Gao Y, Yaegashi J, Zucker JD, Munoz N, Zink EM, Burnum-Johnson KE, Baker SE, Simmons BA, Skerker JM, Gladden JM, Magnuson JK (2021) Multi-omics driven metabolic network reconstruction and analysis of lignocellulosic carbon utilization in *Rhodosporidium toruloides*. *Front Bioeng Biotechnol* 8:612832. <https://doi.org/10.3389/fbioe.2020.612832>
- Koh CMJ, Liu Y, Du Moehninsi, M, Ji L (2014) Molecular characterization of KU70 and KU80 homologues and exploitation of a KU70-deficient mutant for improving gene deletion frequency in *Rhodosporidium toruloides*. *BMC Microbiol* 14:50. <https://doi.org/10.1186/1471-2180-14-50>
- Labuhn M, Adams FF, Ng M, Knoess S, Schambach A, Charpentier EM, Schwarzer A, Mateo JL, Klusmann J-H, Heckl D (2018) Refined sgRNA efficacy prediction improves large- and small-scale CRISPR-Cas9 applications. *Nucleic Acids Res* 46:1375–1385. <https://doi.org/10.1093/nar/gkx1268>
- Liu X-Y, Chi Z, Liu G-L, Madzak C, Chi Z-M (2013) Both decrease in ACL1 gene expression and increase in ICL1 gene expression in marine-derived yeast *Yarrowia lipolytica* expressing INU1

- gene enhance citric acid production from inulin. *Mar Biotechnol* 15:26–36. <https://doi.org/10.1007/s10126-012-9452-5>
- Liu X, Zhang Y, Liu H, Jiao X, Zhang Q, Zhang S, Zhao ZK (2019) RNA interference in the oleaginous yeast *Rhodosporidium toruloides*. *FEMS Yeast Res* 19:foz031. <https://doi.org/10.1093/femsy/foz031>
- Liu J, Zhang S, Li W, Wang G, Xie Z, Cao W, Gao W, Liu H (2023) Engineering a phosphoketolase pathway to supplement cytosolic acetyl-CoA in *Aspergillus niger* enables a significant increase in citric acid production. *J Fungi* 9:504. <https://doi.org/10.3390/jof9050504>
- Lööke M, Kristjuhan K, Kristjuhan A (2011) Extraction of genomic DNA from yeasts for PCR-based applications. *Biotechniques* 50:325–328. <https://doi.org/10.2144/000113672>
- Lopes HJS, Bonturi N, Kerkhoven EJ, Miranda EA, Lahtvee P-J (2020) C/N ratio and carbon source-dependent lipid production profiling in *Rhodotorula toruloides*. *Appl Microbiol Biotechnol* 104:2639–2649. <https://doi.org/10.1007/s00253-020-10386-5>
- Monteiro de Oliveira P, Aborneva D, Bonturi N, Lahtvee P-J (2021) Screening and growth characterization of non-conventional yeasts in a hemicellulosic hydrolysate. *Front Bioeng Biotechnol* 9. <https://doi.org/10.3389/fbioe.2021.659472>
- Niehus X, Crutz-Le Coq A-M, Sandoval G, Nicaud J-M, Ledesma-Amaro R (2018) Engineering *Yarrowia lipolytica* to enhance lipid production from lignocellulosic materials. *Biotechnol Biofuels* 11:11. <https://doi.org/10.1186/s13068-018-1010-6>
- Nowrousian M, Masloff S, Pöggeler S, Kück U (1999) Cell differentiation during sexual development of the fungus *Sordaria macrospora* requires ATP citrate lyase activity. *Mol Cell Biol* 19:450–460. <https://doi.org/10.1128/MCB.19.1.450>
- Nowrousian M, Kück U, Loser K, Weltring K-M (2000) The fungal acl1 and acl2 genes encode two polypeptides with homology to the N- and C-terminal parts of the animal ATP citrate lyase polypeptide. *Curr Genet* 37:189–193. <https://doi.org/10.1007/s002940050518>
- Osorio-González CS, Saini R, Hegde K, Brar SK, Avalos Ramírez A (2022a) Furfural degradation and its effect on *Rhodosporidium toruloides*-1588 during microbial growth and lipid accumulation. *Bioresour Technol* 359:127496. <https://doi.org/10.1016/j.biortech.2022.127496>
- Osorio-González CS, Saini R, Hegde K, Brar SK, Lefebvre A, Avalos-Ramírez A (2022b) Inhibitor degradation by *Rhodosporidium toruloides* NRRL 1588 using undetoxified wood hydrolysate as a culture media. *Biomass Bioenergy* 160:106419. <https://doi.org/10.1016/j.biombioe.2022.106419>
- Otoupal PB, Ito M, Arkin AP, Magnuson JK, Gladden JM, Skerker JM (2019) Multiplexed CRISPR-Cas9-based genome editing of *Rhodosporidium toruloides*. *mSphere* 4:e00099–19. <https://doi.org/10.1128/mSphere.00099-19>
- Pant A, Brahim Belhaouari D, Dsouza L, Yang Z (2023) Upregulation of ATP citrate lyase phosphorylation and neutral lipid synthesis through viral growth factor signaling during vaccinia virus infection. *Eur J Lipid Sci Technol* 113:1031–1051. <https://doi.org/10.1002/ejlt.201100014>
- Pierce MW, Palmer JL, Keutmann HT, Avruch J (1981) ATP-citrate lyase. Structure of a tryptic peptide containing the phosphorylation site directed by glucagon and the cAMP-dependent protein kinase. *J Biol Chem* 256:8867–8870. [https://doi.org/10.1016/S0021-9258\(19\)52474-7](https://doi.org/10.1016/S0021-9258(19)52474-7)
- Pietrocola F, Galluzzi L, Bravo-San Pedro JM, Madeo F, Kroemer G (2015) Acetyl coenzyme A: a central metabolite and second messenger. *Cell Metab* 21:805–821. <https://doi.org/10.1016/j.cmet.2015.05.014>
- Pinheiro MJ, Bonturi N, Belouah I, Miranda EA, Lahtvee P-J (2020) Xylose metabolism and the effect of oxidative stress on lipid and carotenoid production in *Rhodotorula toruloides*: insights for future biorefinery. *Front Bioeng Biotechnol* 8:1008. <https://doi.org/10.3389/fbioe.2020.01008>
- Probst KV, Schulte LR, Durrett TP, Rezac ME, Vadlani PV (2016) Oleaginous yeast: a value-added platform for renewable oils. *Crit Rev Biotechnol* 36:942–955. <https://doi.org/10.3109/0738551.2015.1064855>
- Pronk JT, Yde Steensma H, Van Dijken JP (1996) Pyruvate metabolism in *Saccharomyces cerevisiae*. *Yeast* 12:1607–1633. [https://doi.org/10.1002/\(SICI\)1097-0061\(199612\)12:16%3c1607::AID-YEA70%3e3.0.CO;2-4](https://doi.org/10.1002/(SICI)1097-0061(199612)12:16%3c1607::AID-YEA70%3e3.0.CO;2-4)
- Qiao K, Wasylenko TM, Zhou K, Xu P, Stephanopoulos G (2017) Lipid production in *Yarrowia lipolytica* is maximized by engineering cytosolic redox metabolism. *Nat Biotechnol* 35:173–177. <https://doi.org/10.1038/nbt.3763>
- Ratledge C (2004) Fatty acid biosynthesis in microorganisms being used for single cell oil production. *Biochimie* 86:807–815. <https://doi.org/10.1016/j.biochi.2004.09.017>
- Ratledge C, Wynn JP (2002) The biochemistry and molecular biology of lipid accumulation in oleaginous microorganisms. In: *Advances in Applied Microbiology*. Elsevier, pp 1–52
- Rebnegger C, Graf AB, Valli M, Steiger MG, Gasser B, Maurer M, Mattanovich D (2014) In *Pichia pastoris*, growth rate regulates protein synthesis and secretion, mating and stress response. *Bio-technol J* 9:511–525. <https://doi.org/10.1002/biot.201300334>
- Rekëna A, Pinheiro MJ, Bonturi N, Belouah I, Tammekivi E, Herodes K, Kerkhoven EJ, Lahtvee P-J (2023) Genome-scale metabolic modeling reveals metabolic trade-offs associated with lipid production in *Rhodotorula toruloides*. *PLOS Comput Biol* 19:e1011009. <https://doi.org/10.1371/journal.pcbi.1011009>
- Rhee J, Solomon LA, DeKoter RP (2019) A role for ATP citrate lyase in cell cycle regulation during myeloid differentiation. *Blood Cells Mol Dis* 76:82–90. <https://doi.org/10.1016/j.bcmd.2019.02.006>
- Saini R, Hegde K, Brar SK, Vezina P (2020) Advanced biofuel production and road to commercialization: an insight into bioconversion potential of *Rhodosporidium* sp. *Biomass Bioenergy* 132:105439. <https://doi.org/10.1016/j.biombioe.2019.105439>
- Sato R, Ara S, Yamazaki H, Ishiya K, Aburatani S, Takaku H (2021) Citrate-mediated Acyl-CoA synthesis is required for the promotion of growth and triacylglycerol production in oleaginous yeast *Lipomyces starkeyi*. *Microorganisms* 9:1693. <https://doi.org/10.3390/microorganisms9081693>
- Schultz JC, Cao M, Zhao H (2019) Development of a CRISPR/Cas9 system for high efficiency multiplexed gene deletion in *Rhodosporidium toruloides*. *Biotechnol Bioeng* 116:2103–2109. <https://doi.org/10.1002/bit.27001>
- Schultz JC, Mishra S, Gaither E, Mejia A, Dinh H, Maranas C, Zhao H (2022) Metabolic engineering of *Rhodotorula toruloides* IFO0880 improves C16 and C18 fatty alcohol production from synthetic media. *Microb Cell Factories* 21:26. <https://doi.org/10.1186/s12934-022-01750-3>
- Sreeharsha RV, Mohan SV (2020) Obscure yet promising oleaginous yeasts for fuel and chemical production. *Trends Biotechnol* 38:873–887. <https://doi.org/10.1016/j.tibtech.2020.02.004>
- Stemmer M, Thumberger T, Del Sol KM, Wittbrodt J, Mateo JL (2015) CCTop: an intuitive, flexible and reliable CRISPR/Cas9 target prediction tool. *PLoS ONE* 10:e0124633. <https://doi.org/10.1371/journal.pone.0124633>
- Sukhija PS, Palmquist DL (1988) Rapid method for determination of total fatty acid content and composition of feedstuffs and feces. *J Agric Food Chem* 36:1202–1206. <https://doi.org/10.1021/jf00084a019>

- Sunder S, Gupta A, Kataria R, Ruhal R (2024) Potential of *Rhodosporidium toruloides* for fatty acids production using lignocellulose biomass. *Appl Biochem Biotechnol* 196:2881–2900. <https://doi.org/10.1007/s12010-023-04681-w>
- Takahashi H, McCaffery JM, Irizarry RA, Boeke JD (2006) Nucleocytosolic acetyl-coenzyme A synthetase is required for histone acetylation and global transcription. *Mol Cell* 23:207–217. <https://doi.org/10.1016/j.molcel.2006.05.040>
- Tehlivets O, Scheuringer K, Kohlwein SD (2007) Fatty acid synthesis and elongation in yeast. *Biochim Biophys Acta BBA - Mol Cell Biol Lipids* 1771:255–270. <https://doi.org/10.1016/j.bbalip.2006.07.004>
- Tingajeva O (2024) *Rhodotorula toruloides'* exopolysaccharides: production, optimization and characterization. Tallinn University of Technology, Thesis
- Tiukova IA, Brandenburg J, Blomqvist J, Sampels S, Mikkelsen N, Skaugen M, Arntzen MØ, Nielsen J, Sandgren M, Kerkhoven EJ (2019a) Proteome analysis of xylose metabolism in *Rhodotorula toruloides* during lipid production. *Biotechnol Biofuels* 12:137. <https://doi.org/10.1186/s13068-019-1478-8>
- Tiukova IA, Prigent S, Nielsen J, Sandgren M, Kerkhoven EJ (2019b) Genome-scale model of *Rhodotorula toruloides* metabolism. *Biotechnol Bioeng* 116:3396–3408. <https://doi.org/10.1002/bit.27162>
- Tsai Y-Y, Ohashi T, Kanazawa T, Polburee P, Misaki R, Limtong S, Fujiyama K (2017) Development of a sufficient and effective procedure for transformation of an oleaginous yeast, *Rhodosporidium toruloides* DMKU3-TK16. *Curr Genet* 63:359–371. <https://doi.org/10.1007/s00294-016-0629-8>
- Verduyn C, Postma E, Scheffers WA, Van Dijken JP (1992) Effect of benzoic acid on metabolic fluxes in yeasts: a continuous-culture study on the regulation of respiration and alcoholic fermentation. *Yeast* 8:501–517. <https://doi.org/10.1002/yea.320080703>
- Wang Y, Zhang S, Zhu Z, Shen H, Lin X, Jin X, Jiao X, Zhao ZK (2018) Systems analysis of phosphate-limitation-induced lipid accumulation by the oleaginous yeast *Rhodosporidium toruloides*. *Biotechnol Biofuels* 11:148. <https://doi.org/10.1186/s13068-018-1134-8>
- Wasyleko TM, Ahn WS, Stephanopoulos G (2015) The oxidative pentose phosphate pathway is the primary source of NADPH for lipid overproduction from glucose in *Yarrowia lipolytica*. *Metab Eng* 30:27–39. <https://doi.org/10.1016/j.ymben.2015.02.007>
- Wu S, Hu C, Jin G, Zhao X, Zhao ZK (2010) Phosphate-limitation mediated lipid production by *Rhodosporidium toruloides*. *Biore sour Technol* 101:6124–6129. <https://doi.org/10.1016/j.biotech.2010.02.111>
- Wu S, Zhao X, Shen H, Wang Q, Zhao ZK (2011) Microbial lipid production by *Rhodosporidium toruloides* under sulfate-limited conditions. *Bioresour Technol* 102:1803–1807. <https://doi.org/10.1016/j.biotech.2010.09.033>
- Wu C-C, Honda K, Kazuhito F (2023) Current advances in alteration of fatty acid profile in *Rhodotorula toruloides*: a mini-review. *World J Microbiol Biotechnol* 39:234. <https://doi.org/10.1007/s11274-023-03595-3>
- Wynn JP, Ratledge C (1997) Malic enzyme is a major source of NADPH for lipid accumulation by *Aspergillus Nidulans*. *Microbiology* 143:253–257. <https://doi.org/10.1099/00221287-143-1-253>
- Wynn JP, Kendrick A, Ratledge C (1997) Sesamol as an inhibitor of growth and lipid metabolism in *Mucor circinelloides* via its action on malic enzyme. *Lipids* 32:605–610. <https://doi.org/10.1007/s11745-997-0077-1>
- Wynn JP, Ratledge C, Hamid AA, Li Y (2001) Biochemical events leading to the diversion of carbon into storage lipids in the oleaginous fungi *Mucor circinelloides* and *Mortierella alpina*. *Microbiology* 147:2857–2864. <https://doi.org/10.1099/00221287-147-147-2857>
- Xu P, Qiao K, Ahn WS, Stephanopoulos G (2016) Engineering *Yarrowia lipolytica* as a platform for synthesis of drop-in transportation fuels and oleochemicals. *Proc Natl Acad Sci* 113:10848–10853. <https://doi.org/10.1073/pnas.1607295113>
- Yang F, Zhang S, Zhou YJ, Zhu Z, Lin X, Zhao ZK (2012) Characterization of the mitochondrial NAD<sup>+</sup>-dependent isocitrate dehydrogenase of the oleaginous yeast *Rhodosporidium toruloides*. *Appl Microbiol Biotechnol* 94:1095–1105. <https://doi.org/10.1007/s00253-011-3820-3>
- Yang X, Sun W, Shen H, Zhang S, Jiao X, Zhao ZK (2018) Expression of phosphotransacetylase in *Rhodosporidium toruloides* leading to improved cell growth and lipid production. *RSC Adv* 8:24673–24678. <https://doi.org/10.1039/C8RA03028F>
- Yoon SH, Park JS, Rhee JS (1984) Production of NADPH for Lipogenesis in Oleaginous Yeast Rhodotorula glutinis 12:247–251
- Yu Y, Shi S (2023) Development and perspective of *Rhodotorula toruloides* as an efficient cell factory. *J Agric Food Chem* 71:1802–1819. <https://doi.org/10.1021/acs.jafc.2c07361>
- Zhang Y, Adams IP, Colin R (2007) Malic enzyme: the controlling activity for lipid production? Overexpression of malic enzyme in *Mucor circinelloides* leads to a 2.5-fold increase in lipid accumulation. *Microbiology* 153:2013–2025. <https://doi.org/10.1099/mic.0.2006/002683-0>
- Zhang H, Zhang L, Chen H, Chen YQ, Ratledge C, Song Y, Chen W (2013) Regulatory properties of malic enzyme in the oleaginous yeast, *Yarrowia lipolytica*, and its non-involvement in lipid accumulation. *Biotechnol Lett* 35:2091–2098. <https://doi.org/10.1007/s10529-013-1302-7>
- Zhang H, Zhang L, Chen H, Chen YQ, Chen W, Song Y, Ratledge C (2014) Enhanced lipid accumulation in the yeast *Yarrowia lipolytica* by over-expression of ATP: citrate lyase from *Mus musculus*. *J Biotechnol* 192:78–84. <https://doi.org/10.1016/j.jbiotec.2014.10.004>
- Zhang S, Ito M, Skerker JM, Arkin AP, Rao CV (2016a) Metabolic engineering of the oleaginous yeast *Rhodosporidium toruloides* IFO0880 for lipid overproduction during high-density fermentation. *Appl Microbiol Biotechnol* 100:9393–9405. <https://doi.org/10.1007/s00253-016-7815-y>
- Zhang S, Skerker JM, Rutter CD, Maurer MJ, Arkin AP, Rao CV (2016b) Engineering *Rhodosporidium toruloides* for increased lipid production. *Biotechnol Bioeng* 113:1056–1066. <https://doi.org/10.1002/bit.25864>
- Zhang Y, Kamal R, Li Q, Yu X, Wang Q, Zhao ZK (2022) Comparative fatty acid compositional profiles of *Rhodotorula toruloides* haploid and diploid strains under various storage conditions. *Fermentation* 8:467. <https://doi.org/10.3390/fermentation8090467>
- Zhao Y, Song B, Li J, Zhang J (2022) *Rhodotorula toruloides*: an ideal microbial cell factory to produce oleochemicals, carotenoids, and other products. *World J Microbiol Biotechnol* 38:13. <https://doi.org/10.1007/s11274-021-03201-4>
- Zhu Z, Zhang S, Liu H, Shen H, Lin X, Yang F, Zhou YJ, Jin G, Ye M, Zou H, Zhao ZK (2012) A multi-omic map of the lipid-producing yeast *Rhodosporidium toruloides*. *Nat Commun* 3:1112. <https://doi.org/10.1038/ncomms2112>
- Zhu J, Gu Y, Yan Y, Ma J, Sun X, Xu P (2023) Knocking out central metabolism genes to identify new targets and alternating substrates to improve lipid synthesis in *Y. lipolytica*. *Front Bioeng Biotechnol* 11:1098116. <https://doi.org/10.3389/fbioe.2023.1098116>

**Publisher's Note** Springer Nature remains neutral with regard to jurisdictional claims in published maps and institutional affiliations.